

NATIONAL RADIO ASTRONOMY OBSERVATORY  
CHARLOTTESVILLE, VIRGINIA

ELECTRONICS DIVISION INTERNAL REPORT No. 258

COMPUTER-AIDED TESTING OF MILLIMETER-WAVE MIXERS

MAREK T. FABER AND JOHN W. ARCHER

AUGUST 1985

NUMBER OF COPIES: 125

# COMPUTER-AIDED TESTING OF MILLIMETER-WAVE MIXERS

Marek T. Faber and John W. Archer

## TABLE OF CONTENTS

I.	Introduction . . . . .	1
II.	Derivation of Measurement Formulas . . . . .	2
	A. Effect of Loss in R.F. Components . . . . .	7
	B. Effect of Loss in I.F. Cable . . . . .	9
	1. Lossless I.F. Cable . . . . .	9
	2. Lossy I.F. Cable . . . . .	11
III.	Computer Controlled Measurement Systems . . . . .	15
IV.	Operation of the Measurement System . . . . .	22
	A. Measurements During Cooling or Warming of a Mixer . . . . .	22
	B. Measurements at Constant Temperature . . . . .	28
V.	Discussion of the Results . . . . .	35
VI.	Summary . . . . .	42
VII.	Acknowledgements . . . . .	42

## FIGURES

Fig. 1	Noise Temperature Relationships for a Linear Two-Port Device . . . . .	3
Fig. 2	General Measurement Setup . . . . .	6
Fig. 3	Simplified Block Diagram of the Measurement System . . . . .	16
Fig. 4	Simplified Diagram of Computer-Controlled 1-2 GHz Radiometer/Reflectometer . . . . .	20
Fig. 5	Block Diagram of Software Controlling Measurements and Data Processing During Cooling or Warming of Mixer . . . . .	23
Fig. 6	Photograph of Mixer . . . . .	26
Fig. 7	Schematic Diagram Showing Details of Mixer Design . . . . .	27
Fig. 8	Plots Produced During Cooling of Mixer . . . . .	29
Fig. 9	Plots Resulting From Processing Data During Cooldown . . . . .	30
Fig. 10	Block Diagram of Software Controlling Measurements and Data Processing at Constant Temperature . . . . .	32
Fig. 11	Single-Sideband Mixer Noise Temperature and Corresponding Conversion Loss as a Function of L.O. Level . . . . .	34
Fig. 12	Single-Sideband Mixer Noise Temperature and Corresponding Conversion Loss Versus I.F. Frequency . . . . .	37
Fig. 13	Single-Sideband Mixer Noise Temperature and Corresponding Conversion Loss Versus L.O. Frequency . . . . .	38

## TABLES

Table I	R.F. Performance of the Fixed-Tuned Mixer . . . . .	36
Table II	Comparison of Mixer Performance With Limits Imposed on Schottky Diode Mixer . . . . .	41
References	. . . . .	43

# COMPUTER-AIDED TESTING OF MILLIMETER-WAVE MIXERS

Marek T. Faber and John W. Archer

## I. Introduction

Accurate testing of microwave mixers has been an important problem in mixer development for more than 40 years. Advances in microwave receiver technology have resulted in high sensitivity receivers becoming practical at increasingly higher frequencies. The need for low-noise mixers, especially in the field of millimeter-wave radio astronomy, has stimulated a considerable amount of research into the theory, design and development of mixers and mixer diodes. To achieve improved mixer designs required more accurate measurement methods and more complete testing and characterization of mixers. The lack of coherent signal generators with a known output power at millimeter-wave frequencies resulted in the adoption of measurement methods [1] requiring the use of noise sources only. These methods came into use in the late sixties and were used for simultaneous measurements of gain and noise of amplifiers at lower microwave frequencies. Utilization of hot (at room temperature) and cold (at liquid nitrogen temperature) matched RF loads as noise sources allowed these methods to be utilized in millimeter-wave mixer measurements [2] and resulted in a noise temperature meter which was used in fundamental work on cryogenic cooling of mixers [3]. Measurement setups that evolved from this early design were then successfully used in further development of millimeter-wave, low-noise Schottky diode mixers (e.g., [4], [5], [6], [7], [8], [9], [10]). Although coherent signal generators were still sometimes used either for conversion loss measurements [11] or as a "narrow band noise source" [12], millimeter-wave mixer testing has usually been carried out using the hot and cold load measurement technique (in various forms, e.g., [13], [14]) because of its inherent simplicity, accuracy and speed.

In the late seventies, researchers began to use desktop computers to process data and account for many systematic effects that were very time consuming to correct without the aid of a computer, and were often accepted as measurement errors.

The measurement systems reported in this paper employ a computer not only for processing data but also for controlling the operation of the test apparatus. This approach allows the user to carry out a much more extensive set of mixer performance tests, as well as to obtain data that could not be measured without the aid of high speed, real time system control and data processing. The computer controlled instrument provides a more accurate, reliable, versatile and efficient means of testing and developing millimeter-wave mixers than previously available.

The theoretical basis for the hot and cold load measurement is reviewed in Section II where formulas utilized in the data processing software are derived. Misunderstandings and misinterpretations commonly found in reported measurements of millimeter-wave mixers are clarified. The hardware and software used in the measurement systems is described in Sections III and IV, respectively. Computer printouts that resulted from the testing of a sample mixer are used in Section IV to illustrate the operation of the measurement system and to show the versatility of the test instrument and the variety of data that can be obtained describing mixer performance. The ultra low-noise performance of the mixer is discussed and compared to a shot-noise limit in Section V of the paper.

## II. Derivation of Measurement Formulas

A linear two-port device has, by definition, a linear relationship between input and output signals. In the plot of Figure 1 noise temperature is the input and output quantity. Noise temperature is defined as the ratio of available

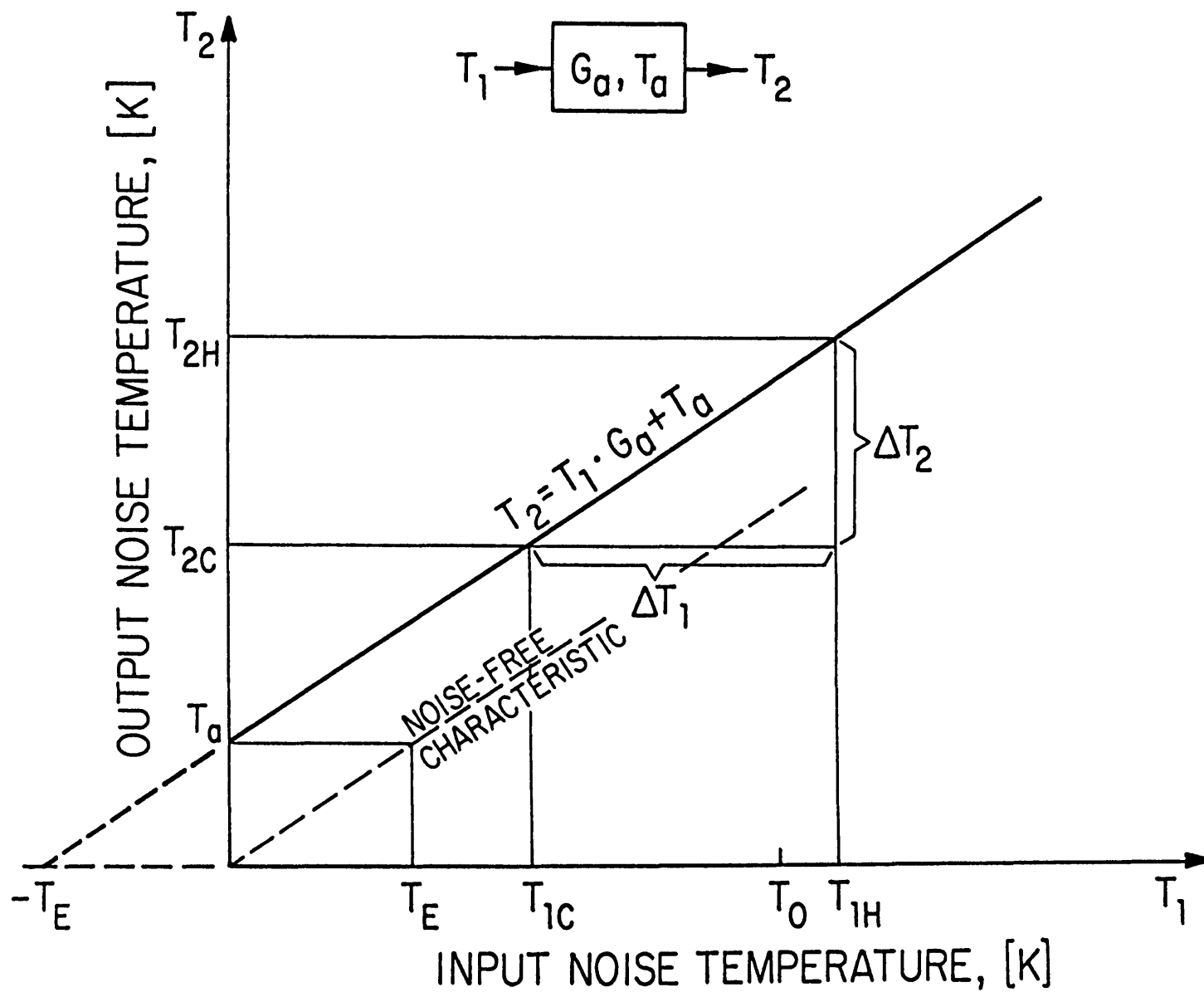


Fig. 1. Noise temperature relationships for a linear two-port device.

noise power spectral density (watts/hertz) to Boltzmann's constant (joules/kelvin) at a specified frequency [1], [17]. By definition, the slope of the line is the available power gain of the two-port:

$$G_a = \frac{\Delta T_2}{\Delta T_1} = \frac{T_{2H} - T_{2C}}{T_{1H} - T_{1C}} = \frac{T_{2C}(Y - 1)}{\Delta T_1} = \frac{T_{2H}(Y - 1)}{Y \Delta T_1} \quad (1)$$

where  $Y = T_{2H}/T_{2C}$  is called the Y-factor. The noise temperature intercept on the output axis,  $T_a = T_2 - T_1 G_a$ , represents the internally generated noise of the two-port and, when referred to the input port, defines the effective input noise temperature:

$$T_E = \frac{T_a}{G_a} = \frac{T_2}{G_a} - T_1 = \frac{T_{1H} - Y T_{1C}}{Y - 1} = \frac{T_{1H} - Y(T_{1H} - \Delta T_1)}{Y - 1} \quad (2)$$

Thus, the effective input noise temperature  $T_E$  is the temperature to which the source conductance of an identical, but noiseless, two-port must be heated in order to provide an available noise power spectral density at the output equal to that generated by the noisy two-port with source conductance at absolute zero temperature.

The spot noise figure [17], [18] can be easily expressed in terms of noise temperatures:

$$\begin{aligned} F &= \frac{T_a + G_a T_o}{G_a T_o} = 1 + \frac{T_E}{T_o} = 1 + \frac{T_{1H} - Y T_{1C}}{T_o(Y - 1)} \\ &= 1 + \frac{\Delta T_1}{T_o(Y - 1)} - \frac{T_{1C}}{T_o} = 1 + \frac{Y \Delta T_1}{T_o(Y - 1)} - \frac{T_{1H}}{T_o} \end{aligned} \quad (3)$$

where  $T_o = 290K$  by convention.

The slope and intercept of the linear transfer characteristic of Figure 1 can be determined from a knowledge of any two points on this line. The gain and noise of a linear two-port device can therefore be determined, for specified input and output frequencies and terminating immittances, by measuring the values of output noise that result from sequentially applying two different known values of input noise. At millimeter-wave frequencies well matched R.F. loads made of absorber formed into a pyramidal shape, are used as input noise sources. Usually one load has a physical temperature of about 295K (room or "hot" load) while the other ("cold" load) is cooled by immersion in liquid nitrogen (77K). Such loads are placed sequentially at the input of a device under test (DUT) and corresponding noise powers at the device output are measured with noise measuring equipment. A system for simultaneous measurements of conversion loss and mixer noise temperature (i.e., effective input noise temperature) of a millimeter-wave cryogenic mixer is shown schematically in Figure 2. The I.F. radiometer/reflectometer is used to measure noise and reflections at the mixer output. Well matched standard hot and cold I.F. loads are used to determine the available power gain  $G_p$  and the effective input noise temperature  $T_p$  of the radiometer at each measurement frequency. The third calibration standard is a short circuit, which is used to calibrate the reflectometer, i.e., to determine noise temperatures  $T_S$  and  $T_S^R = T_S + T_n^R$  of noise waves which are sent outward from the reflectometer when its noise source is turned off and on, respectively. Such a noise measuring system, once calibrated (i.e.,  $G_p$ ,  $T_p$ ,  $T_S$  and  $T_S^R$  are determined), can measure the absolute noise temperature and the magnitude of reflection coefficient of a device connected to its input (port number 3 in Figure 2).

In practical measurements of cryogenically cooled microwave devices neither the input port nor the output port of a mixer is directly accessible and measurements

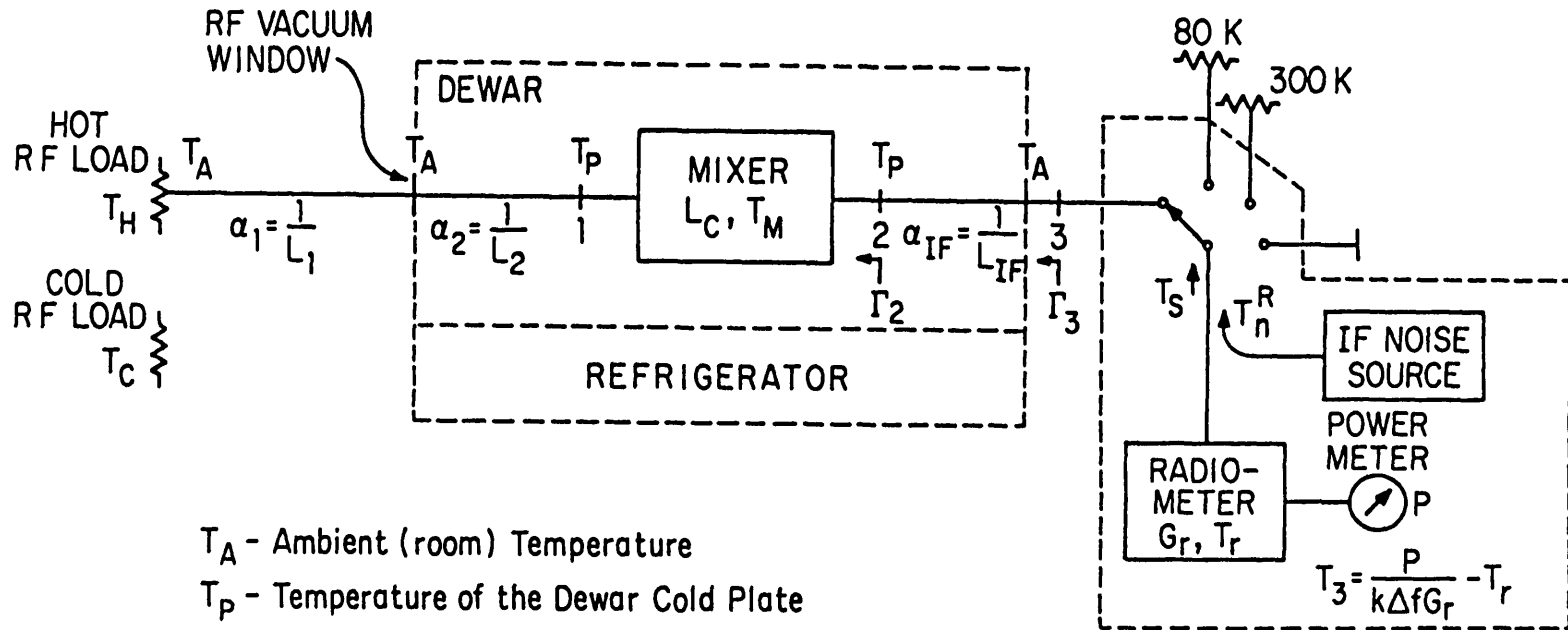


Fig. 2. General measurement setup for simultaneous measurements of the mixer noise temperature and conversion loss of a cryogenic mixer.



have to be made through lossy I.F. cables and R.F. components. It is therefore necessary to develop a model of the measurement system which accounts for these effects and yields corrections which can be applied in order to determine mixer parameters from measured quantities.

A. Effect of Loss in R.F. Components

R.F. and local oscillator signals are usually fed to the mixer input through a quasi-optical or waveguide duplexing system, a dewar vacuum window and, possibly, lossy waveguide components. In the most general case, the R.F. path can be divided into two parts as shown in Figure 2: one, at room temperature ( $T_A$ ), outside the dewar (losses  $L_1$ ;  $\alpha_1 = 1/L_1$ ), and the other (losses  $L_2$ ;  $\alpha_2 = 1/L_2$ ) inside the dewar. The latter guiding structure might have one end at physical temperature  $T_A$  and the other end at the dewar cold plate temperature  $T_P$ .

Because of the loss in the R.F. path, the mixer sees noise temperatures at its input which are different from the hot and cold load temperatures  $T_H$  and  $T_C$ . This is because a lossy R.F. component adds thermal noise power  $P_T = kT_{eq}(1 - 1/L)\Delta f$ , where  $T_{eq}$  is the equivalent temperature which depends on the temperature distribution along the lossy guide [15]. The simplest model assumes a linear distribution and  $T_{eq}$  is then the average of temperatures at device input and output.

Assuming that the matched load at the R.F. system input has temperature  $T_{in}$ , the noise temperature seen by the mixer at port 1 is:

$$\begin{aligned}
 T_1 &= \alpha_2[\alpha_1 T_{in} + (1 - \alpha_1)T_{eq1}] + (1 - \alpha_2)T_{eq2} \\
 &= \alpha_1 \alpha_2 T_{in} + (1 - \alpha_1) \alpha_2 T_A + \frac{1}{2} (1 - \alpha_2)(T_A + T_P)
 \end{aligned} \tag{4}$$

Substituting  $T_{in} = T_C$  for the cold load and  $T_{in} = T_H = T_A$  for the hot load at room temperature:

$$T_{1H} = \alpha_2 T_H + \frac{1}{2} (1 - \alpha_2) (T_H + T_P) \quad (5)$$

$$T_{1C} = \alpha_1 \alpha_2 T_C + (1 - \alpha_1) \alpha_2 T_A + \frac{1}{2} (1 - \alpha_2) (T_A + T_P) \quad (6)$$

The difference in noise temperatures seen by the mixer is determined by  $T_H - T_C$  and the total R.F. losses:

$$\Delta T_1 = T_{1H} - T_{1C} = \alpha_1 \alpha_2 (T_H - T_C) \quad (7)$$

Equation (5) can be rewritten as:

$$T_{1H} = T_H - \frac{1}{2} (1 - \alpha_2) (T_H - T_P) \leq T_H \quad (8)$$

From (5) and (7) it follows that:

$$T_{1C} = T_C + (T_H - T_C) (1 - \alpha_1 \alpha_2) - \frac{1}{2} (1 - \alpha_2) (T_H - T_P) \geq T_C \quad (9)$$

Thus the R.F. losses result in the room temperature load appearing to be colder and the cold load hotter than the true temperatures when measured at the input of a cryogenically cooled mixer. This results in a reduction in the input noise temperature difference by a factor of  $\alpha_1 \alpha_2$ . It is clear, therefore, that in order to preserve the accuracy of mixer parameters measurements, it is essential to keep R.F. input losses to a minimum, consistent with other constraints such as the thermal design of the cryostat.

## B. Effect of Loss in I.F. Cable

In order to derive the corrections to be applied in determining the mixer parameters from measured quantities, first consider the case where the I.F. cable connecting mixer output to radiometer/reflectometer input is lossless, i.e.,  $\alpha_{IF} = 1/L_{IF} = 1$ .

### 1. Lossless I.F. Cable ( $\alpha_{IF} = 1$ )

The noise measured by the I.F. radiometer is composed of the noise delivered from the mixer output into the I.F. cable and the noise transmitted outward from the radiometer and reflected back from the mixer I.F. terminals. Since the two components are uncorrelated, then:

$$T_3 = T_2(1 - |\Gamma_2|^2) + T_S |\Gamma_2|^2 \quad (10)$$

and

$$T_2 = \frac{T_3 - T_S |\Gamma_2|^2}{1 - |\Gamma_2|^2} \quad (11)$$

Thus the only necessary correction is for a mismatch at the mixer output [3], [19].

At each measurement frequency, three noise temperatures need to be measured:

1. Hot load ( $T_{1H}$ ) at mixer input; I.F. reflectometer noise source off

$$T_{3H} = T_{2H} (1 - |\Gamma_2|^2) + T_S |\Gamma_2|^2 \quad (12)$$

2. Hot load ( $T_{1H}$ ) at mixer input; I.F. reflectometer noise source on

$$T_{3H}^R = T_{2H} (1 - |\Gamma_2|^2) + T_S^R |\Gamma_2|^2 \quad (13)$$

3. Cold load ( $T_{1C}$ ) at mixer input; I.F. reflectometer noise source off

$$T_{3C} = T_{2C} (1 - |\Gamma_2|^2) + T_S |\Gamma_2|^2 \quad (14)$$

From these measurements:

$$|\Gamma_2|^2 = \frac{T_{3H}^R - T_{3H}}{T_S^R - T_S} = \frac{T_{3H}^R - T_{3H}}{T_n^R} = |\Gamma_3|^2 \quad (15)$$

and the mixer conversion loss (i.e., ratio of available power of the R.F. source to power delivered to I.F. load):

$$L_c^{DSB} = \frac{\Delta T_1}{\Delta T_3} = \frac{T_{1H} - T_{1C}}{T_{3H} - T_{3C}} \quad (16)$$

Because noise temperatures are defined in terms of available noise power [1], [20], it is necessary to derive an "available conversion loss"  $L_a$ , which corresponds to the available power gain relating output and input noise temperatures (Figure 1).  $L_a$  is defined as the ratio of available power of the R.F. source to available power at the mixer I.F. output. Using (11),  $L_a$  can be expressed as:

$$L_a^{DSB} = \frac{\Delta T_1}{\Delta T_2} = \frac{T_{1H} - T_{1C}}{T_{2H} - T_{2C}} = \frac{T_{1H} - T_{1C}}{T_{3H} - T_{3C}} (1 - |\Gamma_2|^2)$$

or

$$L_a^{DSB} = (1 - |\Gamma_2|^2) \frac{\Delta T_1}{\Delta T_3} = (1 - |\Gamma_2|^2) L_c^{DSB} \quad (17)$$

From (2) the mixer noise temperature (i.e., effective input noise temperature) is then given by:

$$T_M^{DSB} = T_{2H} L_a^{DSB} - T_{1H}$$

$$T_M^{DSB} = (T_{3H} - T_S |\Gamma_2|^2) \frac{\Delta T_1}{\Delta T_3} - T_{1H} \quad (18)$$

For a double sideband mixer [3], [21]:

$$T_M^{SSB} = T_M^{DSB} \left(1 + \frac{L_s}{L_1}\right)$$

and

$$L_c^{SSB} = L_c^{DSB} \left(1 + \frac{L_s}{L_1}\right) \quad (19)$$

which for a broadband mixer having equal conversion losses from both sidebands,  $L_s = L_1$ , gives:

$$T_M^{SSB} = 2T_M^{DSB} \quad \text{and} \quad L_c^{SSB} = 2L_c^{DSB} \quad (20)$$

## 2. Lossy I.F. Cable ( $\alpha_{IF} < 1$ )

The lossy I.F. cable generates thermal noise which adds to the noise at the radiometer input. It has been shown [16] that the noise radiated from the two ends of the lossy cable is uncorrelated, i.e., in Figure 2 the thermal noise power incident on port 3 is not dependent on the phase of the reflection coefficient  $\Gamma_2$ . Thus the I.F. radiometer/reflectometer measures the noise temperature:

$$T_3 = T_2(1 - |\Gamma_2|^2) \alpha_{IF} + T_S |\Gamma_2|^2 \alpha_{IF}^2 + T_T + T_T |\Gamma_2|^2 \alpha_{IF}$$

Because  $T_T = (1 - \alpha_{IF}) T_{ceq}$ , where  $T_{ceq}$  is the equivalent temperature of I.F. cable [15] ( $T_{ceq} = \frac{1}{2} (T_A + T_P)$  for a linear temperature distribution along the cable),

then:

$$T_3 = a_{IF}(1 - |\Gamma_2|^2) T_2 + a_{IF}^2 |\Gamma_2|^2 T_S + (1 - a_{IF})(1 + a_{IF} |\Gamma_2|^2) T_{ceq} \quad (21)$$

$$T_3 = a_{IF}(1 - |\Gamma_2|^2) T_2 + a_{IF}^2 |\Gamma_2|^2 T_S + \delta T_3$$

The noise temperature at the mixer output  $T_2$  can now be expressed as:

$$T_2 = \frac{T_3 - a_{IF}^2 |\Gamma_2|^2 T_S}{a_{IF}(1 - |\Gamma_2|^2)} - \delta T_2 \quad (22)$$

where

$$\delta T_2 = \frac{(1 - a_{IF})(1 + a_{IF} |\Gamma_2|^2)}{a_{IF}(1 - |\Gamma_2|^2)} T_{ceq}$$

When the noise generated in the I.F. cable is taken into account, the noise temperatures (12), (13), (14) measured at each test frequency become:

$$T_{3H} = a_{IF}(1 - |\Gamma_2|^2) T_{2H} + a_{IF}^2 |\Gamma_2|^2 T_S + \delta T_3 \quad (23)$$

$$T_{3H}^R = a_{IF}(1 - |\Gamma_2|^2) T_{2H} + a_{IF}^2 |\Gamma_2|^2 T_S^R + \delta T_3 \quad (24)$$

$$T_{3C} = a_{IF}(1 - |\Gamma_2|^2) T_{2C} + a_{IF}^2 |\Gamma_2|^2 T_S + \delta T_3 \quad (25)$$

From these measurements:

$$a_{IF}^2 |\Gamma_2|^2 = \frac{T_{3H}^R - T_{3H}}{T_S^R - T_S} = |\Gamma_3|^2 \quad (26)$$

Substituting  $|\Gamma_2|^2$  in (21) and (22) gives:

$$T_3 = (a_{IF} - \frac{1}{a_{IF}} |\Gamma_3|^2) T_2 + |\Gamma_3|^2 T_S + \delta T_3 \quad (27)$$

where

$$\delta T_3 = (1 - a_{IF})(1 + \frac{1}{a_{IF}} |\Gamma_3|^2) T_{ceq} \quad (28)$$

and

$$T_2 = \frac{a_{IF}(T_3 - |\Gamma_3|^2 T_S)}{a_{IF}^2 - |\Gamma_3|^2} - \delta T_2 \quad (29)$$

where

$$\delta T_2 = \frac{(1 - a_{IF})(a_{IF} + |\Gamma_3|^2)}{a_{IF}^2 - |\Gamma_3|^2} T_{ceq} \quad (30)$$

The available conversion loss of the mixer can be derived from measured quantities as:

$$L_a^{DSB} = \frac{\Delta T_1}{\Delta T_2} = \frac{T_{1H} - T_{1C}}{T_{2H} - T_{2C}} = \frac{a_{IF}^2 - |\Gamma_3|^2}{a_{IF}} \cdot \frac{T_{1H} - T_{1C}}{T_{3H} - T_{3C}} \quad (31)$$

$$L_a^{DSB} = (a_{IF} - \frac{1}{a_{IF}} |\Gamma_3|^2) \frac{\Delta T_1}{\Delta T_3}$$

Using equation (17) mixer conversion loss is then:

$$L_c^{DSB} = \frac{L_a^{DSB}}{1 - |\Gamma_2|^2} = a_{IF} \frac{\Delta T_1}{\Delta T_3} \quad (32)$$

Mixer noise temperature can be derived in a similar way as in equation (18):

$$T_M^{DSB} = (T_{3H} - |\Gamma_3|^2 T_S) \frac{\Delta T_1}{\Delta T_3} - T_{1H} - \delta T_M \quad (33)$$

where

$$\delta T_M = \delta T_2 L_a^{DSB} = \delta T_2 (1 - |\Gamma_2|^2) L_c^{DSB} \quad (34)$$

which can be expressed in terms of measured quantities as:

$$\delta T_M = (1 - a_{IF}) \left(1 + \frac{1}{a_{IF}} |\Gamma_3|^2\right) T_{ceq} \frac{\Delta T_1}{\Delta T_3} \quad (35)$$

or

$$\delta T_M = \delta T_3 \frac{\Delta T_1}{\Delta T_3}$$

The above derivations clearly show the corrections that need to be applied at each measurement frequency in order to determine mixer conversion loss and mixer noise temperature from the measured quantities  $T_{3H}$ ,  $T_{3H}^R$  and  $T_{3C}$ . The results also indicate sources of potential measurement inaccuracies inherent in the hot/cold load measurement technique employing a calibrated I.F. radiometer/reflectometer to make noise measurements. Clearly, a computer aided measurement system can provide a more accurate, reliable and efficient means of testing and developing millimeter-wave mixers than manual point-by-point measurements. Such a system can also offer tests which are not feasible without aid of a computer. For example, fast and accurate measurements and real-time data processing are indispensable to successfully test mixer during cooling because measurements at a given temperature have to be made in a time, which is short enough for little temperature change to occur.

The formulas derived also indicate which parts of the test system need to be carefully designed and how to optimize system software to minimize measurement errors in various tests.



### III. Computer Controlled Measurement Systems

Two measurement systems have been constructed to allow simultaneous testing of millimeter-wave mixers in two different frequency ranges. One setup covers 90 GHz to 190 GHz in two subranges, while the other is used at frequencies from 200 GHz to 290 GHz and also allows measurements up to 350 GHz. Both setups employ the same cryogenic systems, similar I.F. radiometers/reflectometers, and both are controlled by Apple II+ desktop computers running the same software. The major differences between the systems lie in the design of the quasi-optical diplexers and the local oscillator sources.

A simplified block diagram of the measurement setup is shown in Figure 3. The cryogenic system is a double dewar arrangement devised for a multiple mixer radio astronomy receiver [22]. The refrigerator used to cool the mixer under test is a Cryogenics Technology, Inc. Model 350. The refrigerator head is attached to a vacuum dewar which serves to insulate the cold stations of the system from the ambient environment. The main dewar cold plate is surrounded by a polished and gold-plated shield attached to the 77K station which aids in reducing radiative heat loading on the 12K station. The mixer and I.F. amplifier are mounted in a cryogenic sub-dewar, comprising a separate vacuum chamber and a cold stage which can be readily thermally connected to or disconnected from the main dewar cold plate by a mechanical heat switch. Such an arrangement allows the sub-dewar to be warmed up without turning off the refrigerator. Thus, the mixer can be changed and then rapidly cooled again by closing the heat switch to the cold main dewar plate.

A Teflon lens, which is transparent to millimeter wavelength radiation, matches the diverging radiation pattern of the mixer feed horn to the quasi-collimated beam within the L.O. diplexer and serves as a R.F. vacuum window.

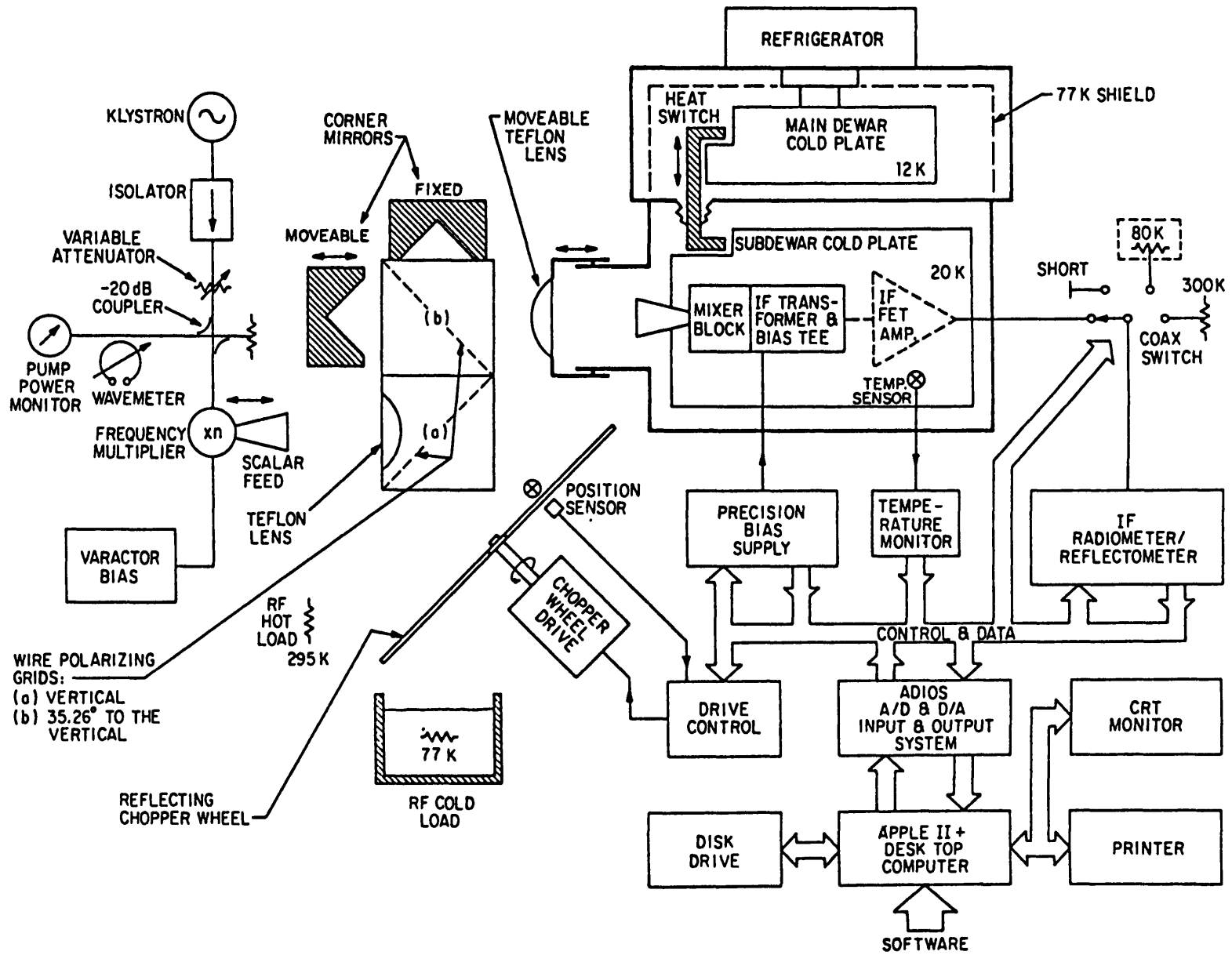


Fig. 3. Simplified block diagram of the measurement system.

Polarizing type duplexers [23] are used in both systems for L.O./R.F. combining and filtering. The higher R.F. frequency duplexer is similar to one described previously [8]. The other duplexer is an implementation of that design scaled down in frequency. The polarizing grids used in the duplexers are free-standing 0.05 mm diameter BeCu wire grids with 75 wires per centimeter mounted on removable forms.

Four different sets of feed horns and lenses give a far-field -11 dB full beam-width of  $4.2^\circ$  independent of frequency in each of the four frequency subranges, namely in 90-120 GHz, 130-190 GHz, 200-290 GHz and 280-360 GHz. The feed horns have a flare angle of  $4.57^\circ$  and are corrugated with the first 10 slots tapered in depth in order to improve the horn SWR and reduce coupling to the  $\text{EH}_{12}$  mode in the throat region [24], [25]. The circular waveguide at the throat of the horn is coupled to a standard rectangular guide via a five-section, quarter-wave transformer.

The circularly symmetric lenses are made from Teflon. The lens is designed on the basis of geometrical optics and is constructed so that the surface towards the feed is plane. The lens thickness, at a given radial distance from the center, was derived from the parametric formulas given in [26]. The lens surfaces are concentrically grooved in order to reduce reflection losses at the air/dielectric interface. The grooves have an easily machined triangular cross section and are designed [27] to result in a power reflection coefficient for the lens of less than 0.01 over the entire frequency subrange. The total loss of the lens, including the effects of dissipation in the dielectric and reflections at the air/dielectric interface is less than 0.15 dB.

The lower R.F. frequency duplexer has a total loss, including lens reflection and feed coupling losses, of less than 0.4 dB when operating with a 1.5 GHz

I.F. The total loss of the higher frequency diplexer operating with the same I.F. is between 0.4 and 0.6 dB at frequencies from 200 to 290 GHz and increases to ~ 0.8 dB at 350 GHz. The diplexers provide more than 20 dB rejection of the local oscillator noise sidebands.

The local oscillator sources used in measurement setups are frequency-multiplied klystrons. Four frequency multipliers have been developed to cover the entire frequency range from 90 GHz to 350 GHz. Crossed-waveguide frequency doublers provide L.O. signal in the two lower frequency subranges [28], [29]. In the frequency range from 200 to 290 GHz an efficient frequency tripler [30] is used. The L.O. source used in measurements at 310 to 350 GHz is a 6x multiplier chain composed of a quasi-optical tripler [31] driven by high output power frequency doublers [32].

R.F. loads made from Eccosorb AN72 formed into a pyramidal shape for minimal error due to reflections from the terminations are used as input noise sources. One load is at room temperature while the other is immersed in liquid nitrogen enclosed in a styrofoam bucket. The diplexer R.F. input beam is switched between the two loads by a rotating reflecting chopper wheel made from aluminum.

D.C. bias from a computer controllable precision bias supply is fed to the mixer under test through an I.F. transformer and bias tee [8] which is integrated with the mixer block. The I.F. output from the transformer is usually connected to the radiometer/reflectometer through a gold-plated, stainless steel, coaxial air line. A low-noise I.F. amplifier [33] can be inserted between transformer output and I.F. line if the performance of the mixer in a receiver configuration is to be tested. The amplifier is mounted on the sub-dewar cold plate close to the mixer and when cooled to 20K has input noise temperature less than 10K

between 1.2 and 1.8 GHz with a gain of 30 dB and an input VSWR of less than 1.4:1 over the same range.

Noise at the sub-dewar I.F. output is measured by a stable, precisely calibrated, computer-controlled 1-2 GHz radiometer/reflectometer mentioned briefly in the preceding section and shown schematically in Figure 4. The remote unit is placed close to the sub-dewar I.F. output in order to minimize the length of the input cable. The unit comprises a noise diode with its driving circuit, a 10 dB attenuator, a 20 dB directional coupler, a circulator and a low-noise 20 dB gain 1-2 GHz amplifier. The noise diode is turned on and off under computer control as required.

The amplified signal is fed into the main radiometer unit where it is further amplified in an additional 20 dB gain 1-2 GHz amplifier. That amplifier can be bypassed if lower radiometer gain is needed (e.g., when receiver tests are to be made). The amplified signal is then converted to a baseband frequency in a double sideband mixer. The local oscillator signal for the conversion is provided by a voltage controlled oscillator tuned from 1 to 2 GHz by a linearizing amplifier/driver under computer control.

The level of the down converted baseband signal can be adjusted in 1 dB steps by an electronically switched attenuator. The attenuator is followed by a low-pass filter whose bandwidth, and thus the noise measurement half bandwidth, can be electronically set to 5, 10, 30, 100 or 250 MHz.

A baseband amplifier provides 20 dB of additional gain before the signal is detected in an accurate square law detector. A D.C. amplifier provides final amplification to the level required by the computer, which completes the signal processing. The radiometer/reflectometer has an effective input noise temperature of about 300K when the 60 MHz measurement bandwidth is selected and is sufficiently stable for recalibration to be required every three or four hours.

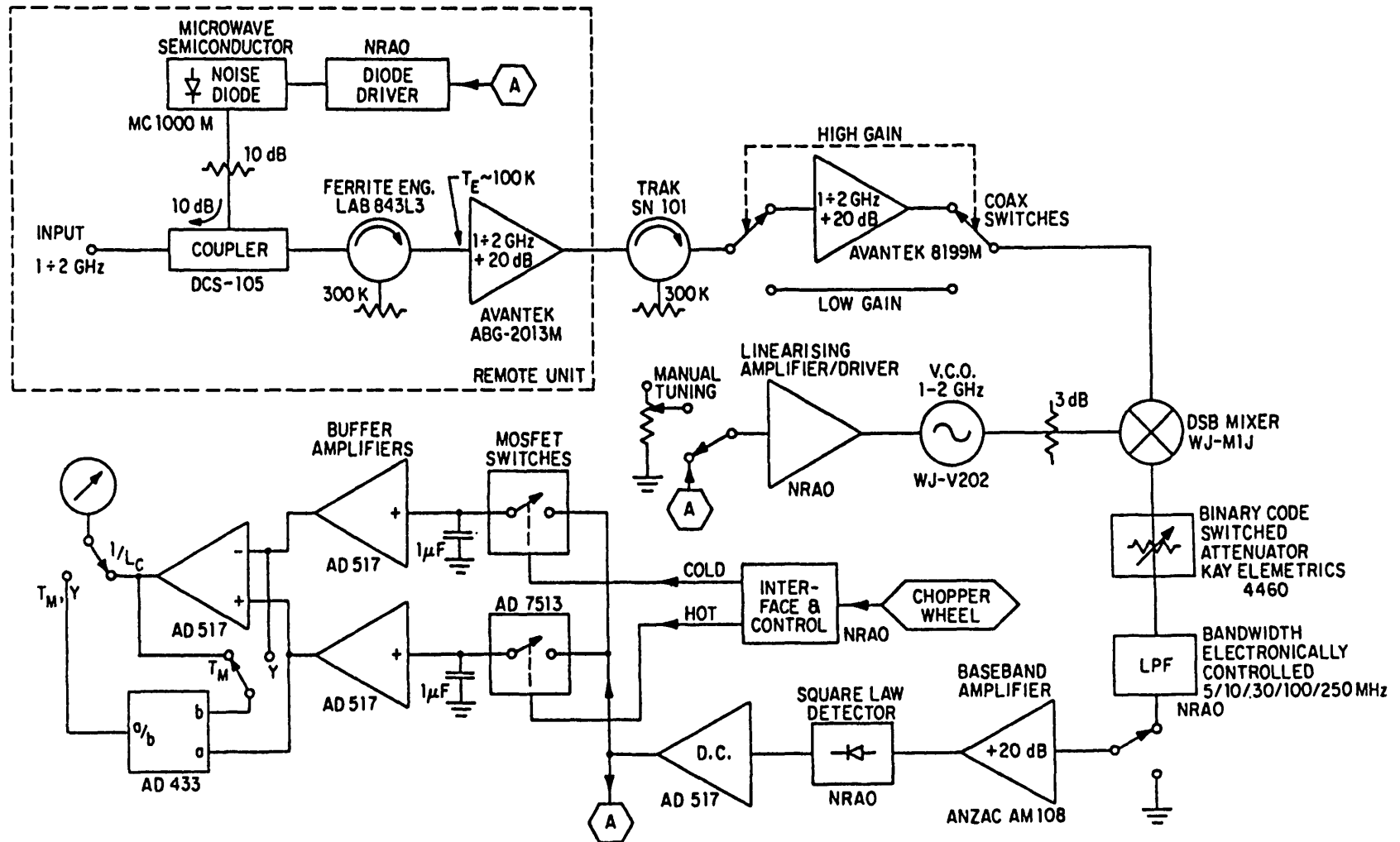


Fig. 4. Simplified diagram of the computer-controlled 1-2 GHz radiometer/reflectometer.  $\odot$  symbol indicates signals coming to or from other components of the measurement system ("A" represents the computer interface input and output system "ADIOS").

The output signal from the D.C. amplifier is also fed to two sample and hold circuits. The sampling switches of these circuits are controlled by "hot" and "cold" TTL level signals indicating the R.F. load seen by the mixer under test at a given instant. These TTL signals are provided by the chopper wheel control circuit. The output signals from the sample and hold circuits are fed through buffer amplifiers into a differential amplifier and an analog divider. A panel meter can be connected to the output of either circuit. Depending on the positions of the switches, the reading of the meter is proportional either to the mixer noise temperature or the Y factor, or to the reciprocal of the mixer conversion loss. Such an arrangement greatly simplifies the optimization of mixer tuning and bias where only relative changes in mixer performance need to be monitored.

An electrically controlled coaxial switch at the radiometer input (Figure 3) is used to select either the mixer (or receiver) output or any of three calibration standards. The short circuit and the well-matched loads which are accurate, absolute standards of noise devised by Weinreb [34] are connected to the switch through coaxial cables of exactly the same length as the fourth (mixer) cable. The radiometer/reflectometer may then be calibrated at the plane of the sub-dewar output connector including the I.F. cable in the radiometer/reflectometer calibration.

The operation of each measurement setup is controlled by Apple II+ desktop computer which is interfaced to the setup through an input and output system ("ADIOS") [35] comprising digital interfaces and analog-to-digital and digital-to-analog converters. User oriented "friendly" interactive software completes the test system.

The computer instructs the user of the system, checks for possible mistakes and helps in presetting a test program. The computer supervises the calibration

of the measurement system and stores the calibration data. When the calibration is completed the computer controls measurements according to the preset test program, collects data and performs in real-time all calculations applying necessary corrections as described in Section II. It also displays and plots parameters of a mixer under test and, if desired, prints out plots and measured quantities. The software and operation of the measurement system is described in more detail in Section IV where results of measurements of an ultra low-noise, fixed-tuned mixer are used to illustrate the test procedure.

#### IV. Operation of the Measurement System

The computer program is divided into four parts to accommodate the software in the 48K byte available memory. Only the part which is needed for particular tests is stored in the computer. The calibration and measurement data is preserved when another part of the program is loaded from the disk.

##### A. Measurements During Cooling or Warming of a Mixer

A simplified block diagram of the software controlling the measurements during cooling or warming is shown in Figure 5. Before starting the measurements, the computer assists the user in setting a test program for the cooldown or warmup. If noise temperature is to be measured the computer checks the radiometer calibration and returns to the main menu if recalibration is needed. The reflectometer calibration completes the calibration procedure required for the noise measurements.

Temperature intervals,  $\Delta T$ , at which measurements are to be made and the lowest (or highest) temperature which sets the limit for the measurements are entered when establishing the test program.  $\Delta T = 0$  disables the temperature monitoring loop and allows measurements to be supervised via the computer keyboard.



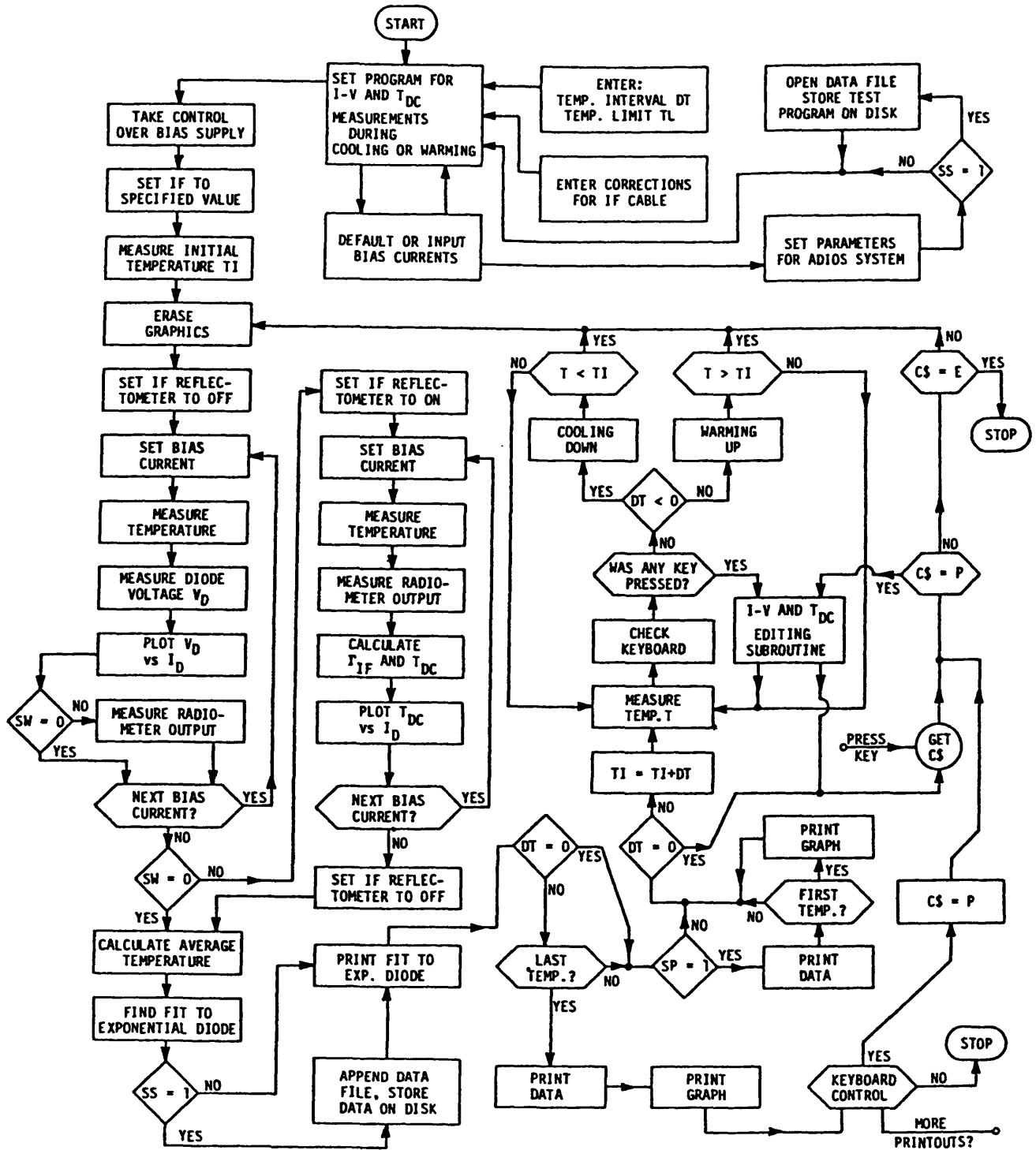


Fig. 5. Simplified block diagram of the software controlling the measurements and data processing during cooling or warming of a mixer. Operation of the system depends on control variables the values of which are set in establishing the test program: SW = 0 - no noise temperature measurements are to be made; SS = 1 - data is to be stored on disk; SP = 1 - full printouts at each temperature.

The measurements may be made either at 21 default values of bias current spread evenly in logarithmic scale or at up to 61 alternative user-specified bias currents in the range from 10 nA to 10 mA. The default I.F. frequency is set by the software to 1.4 GHz but may be changed to any value from 1 GHz to 2 GHz. The test program parameters and the results of measurements may be stored on the disk for further data processing by the computer after the cooling (or warming) is completed.

When the test program is started, the computer takes control over the precision bias supply and the I.F. radiometer/reflectometer and enters a measurement loop. The loop has been carefully optimized to obtain high accuracy of measurements and to minimize the effect of temperature change between the first and the last measurement points. It should be noted that high accuracy and speed of measurement and data processing are essential and can only be achieved with the aid of a computer.

At each temperature the system measures the I-V characteristic of the mixer diode and the equivalent I.F. noise temperature with D.C. bias only,  $T_{DC}^1$ , employing the formulas derived in Section II. The results of measurements and real-time calculations are plotted versus bias current on a CRT monitor. When the measurements at a given temperature are completed the computer attempts to fit the data to a model response of an ideal exponential diode with series resistor [36], [37] (i.e.,  $V_D = V_j + I_D R_s = V_j + R_s I_{sat} [\exp(qV_j/\eta kT) - 1]$ ) using the least squares method. It also computes residuals of the fit and derivatives  $dV_D(I_D)/d \log(I_D)$  and  $dV_j(I_D)/d \log(I_D)$ . These are very useful in characterizing the quality of a Schottky barrier mixer diode and provide more insight into the

---

<sup>1</sup>The measured quantity  $T_{DC}$  includes noise contributions from sources other than just the diode, i.e., from mount losses, and is quite distinct from the noise temperature of the D.C. biased diode [3], [21].

diode performance than the commonly used parameter  $\Delta V = V_D(100 \mu A) - V_D(10 \mu A)$ . Any deviation in the diode I-V characteristic from the exponential response can easily be traced because the latter derivative is independent of  $\log(I_D)$  for the ideal diode. A correlation between the I-V characteristic and an excess noise sometimes present in cooled Schottky diodes can also be studied. Effects of a whisker losing contact with the diode's anode or punching through the diode epilayer can be monitored as the temperature is varied and thus providing indications for diode contacting and mixer assembling.

The results of measurements and data processing, including all the plots, are printed out (or may be printed out on request, depending on the test program) by an editing subroutine which complements the measurement and temperature monitoring loops. The measurements are completed when the mixer temperature reaches the limit specified in the test program. The data stored on the disk may be further processed at a later time to produce plots of the measured diode parameters at specified temperatures or as a function of temperature.

The tests performed on a typical mixer are illustrated in Figures 8 and 9. The mixer, shown in Figures 6 and 7, was a single-ended, fundamental frequency, fixed-tuned mount developed from a design described previously [24]. A whisker contacted Schottky barrier diode (2P9-300 fabricated by R. Mattauch at the University of Virginia) was mounted in reduced height waveguide coupled to the standard WR-8 input waveguide through five-section impedance transformer. In order to obtain low-noise, broadband operation of a fixed-tuned mixer, the whisker length and configuration were empirically selected in such a way that the whisker inductance series resonates the combined capacitance of microstrip R.F. choke and diode at a frequency above the highest mixer operating frequency. In this case, changes in the impedance (capacitive) of the diode/whisker combination compensate

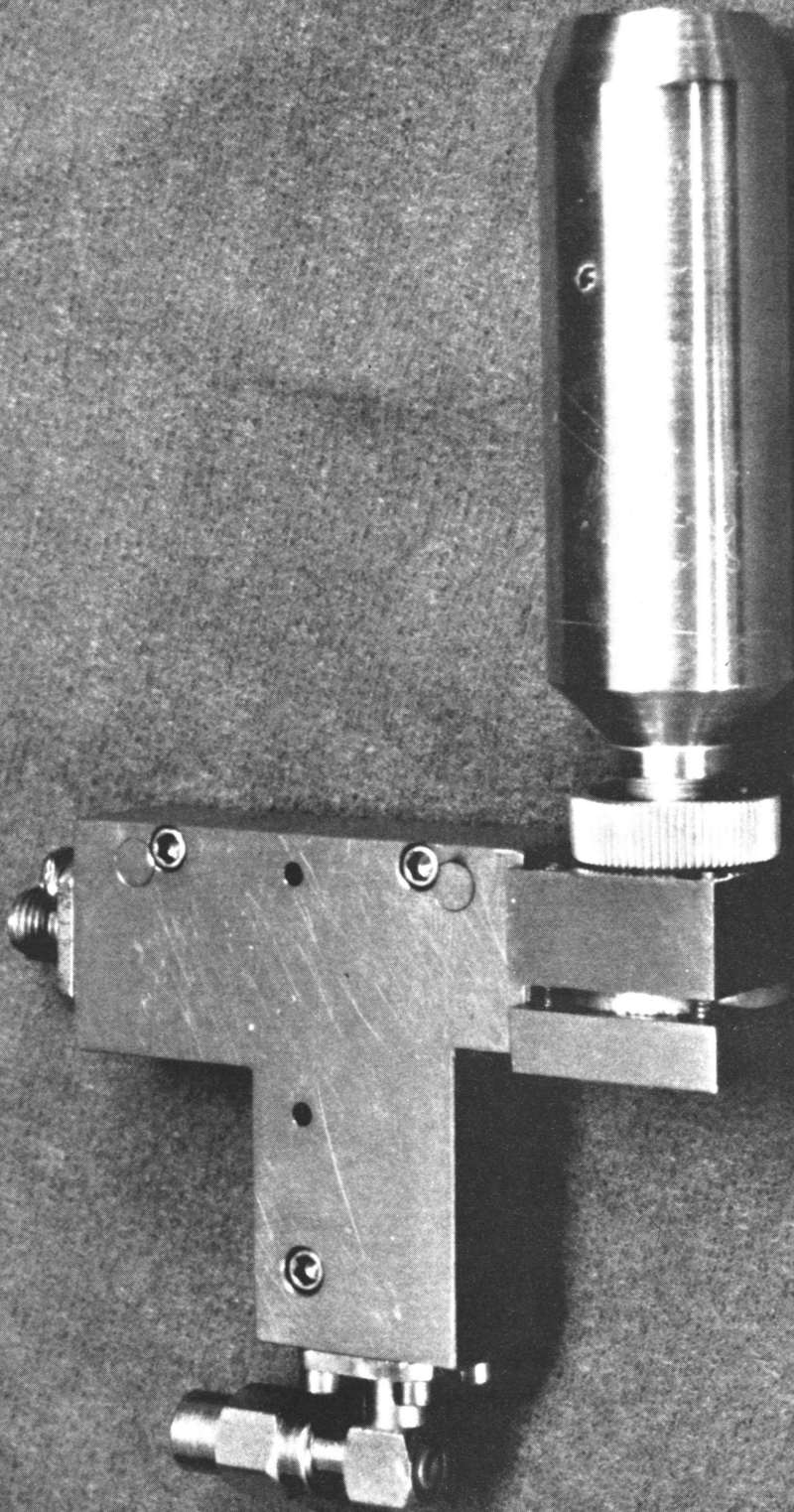
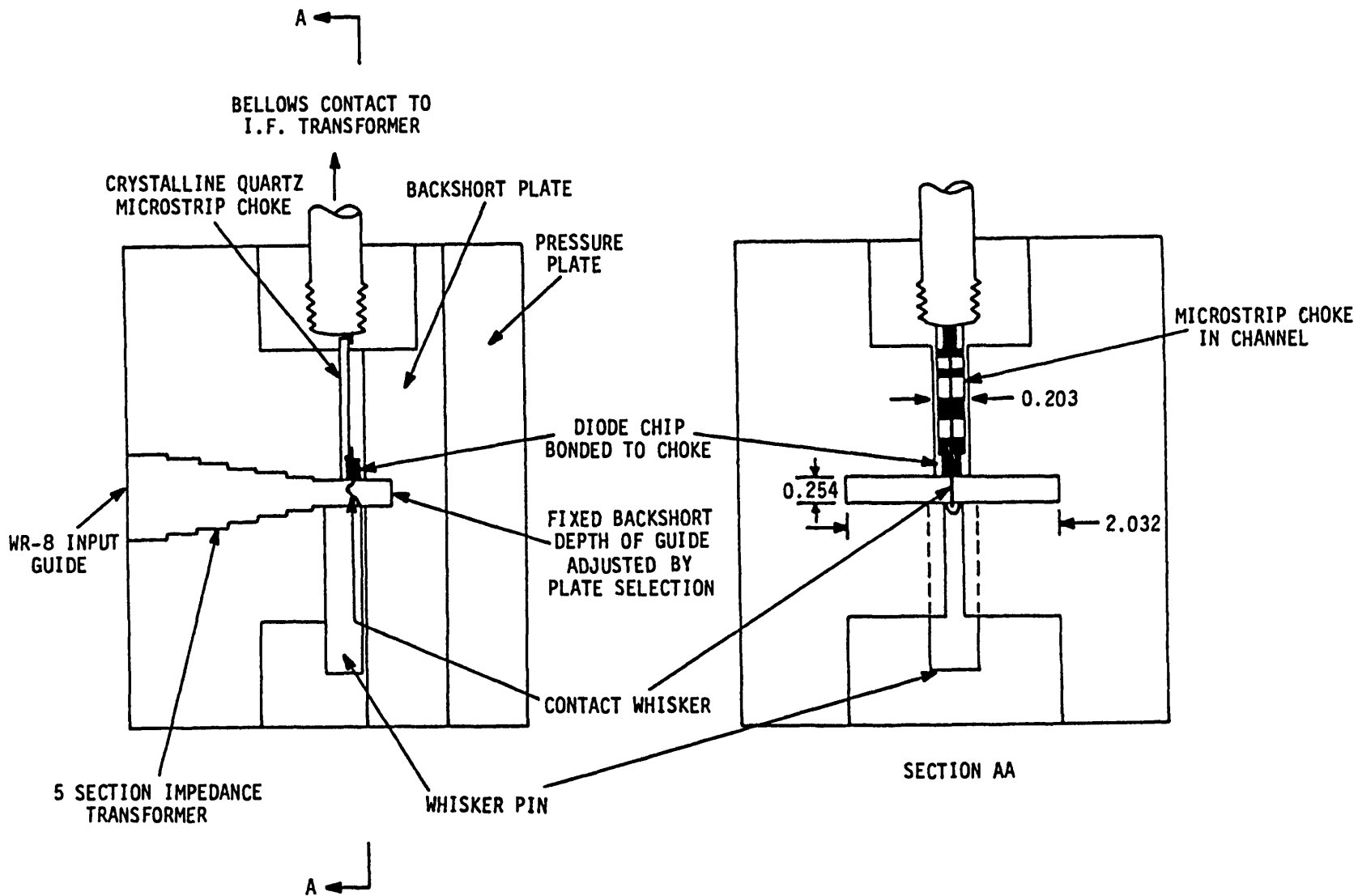


Fig. 6. A photograph of the mixer.



27

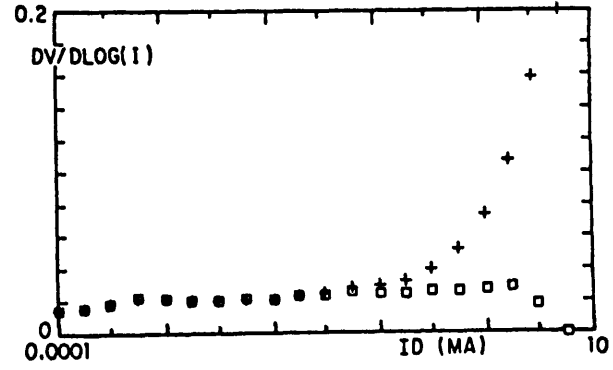
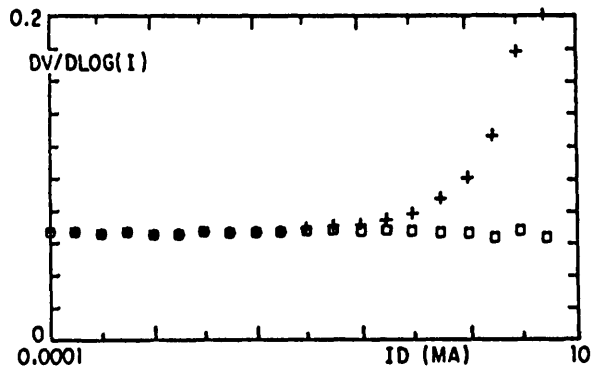
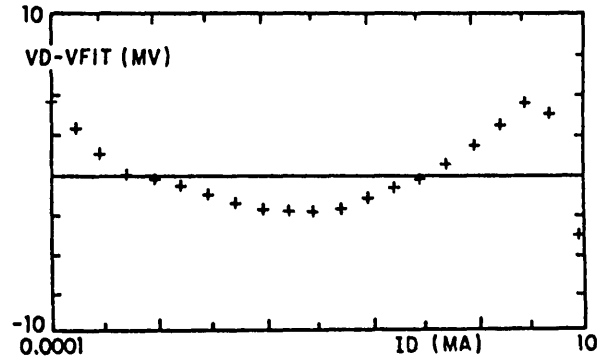
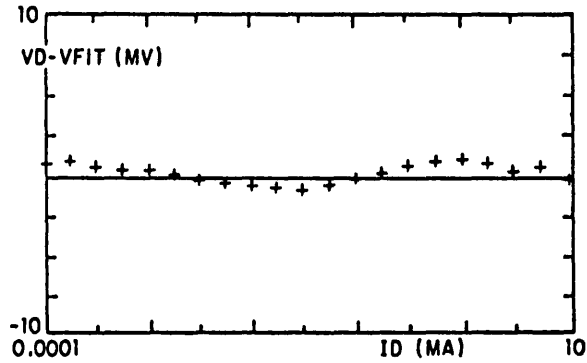
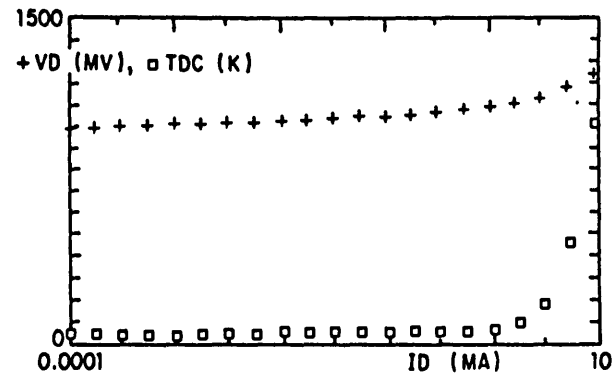
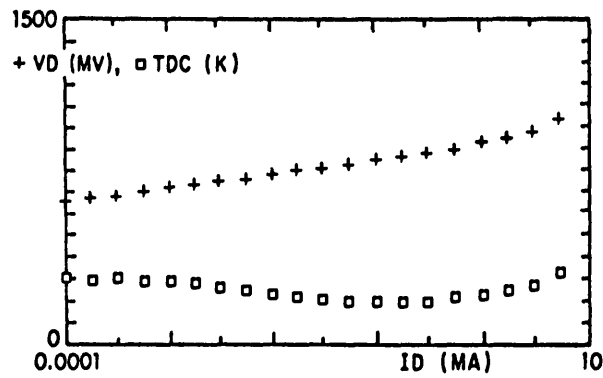
Fig. 7. A schematic diagram (not to scale) showing the details of the mixer design.

for changes of the inductive reactance seen toward the fixed backshort as the frequency is varied.

The plots in Figure 8 were produced during cooling of the mixer to illustrate operation of the measurement system. Plots presented in Figure 9 are the result of processing data collected during cooldown and reflect the changes in diode properties upon cooling. At room temperature the Schottky barrier diode was characterized by a zero bias capacitance  $C_{j0} = 8.0$  fF, a series resistance  $R_s = 11.7 \Omega$ , a saturation current  $I_{sat} = 1.8 \times 10^{-17}$  A,  $\Delta V = 67.6$  mV and an ideality factor  $\eta = 1.14$  ( $V_o = \eta kT/q = 28.7$  mV). The equivalent I.F. noise temperature,  $T_{DC}$ , was 227K and 200K at D.C. bias currents of 10  $\mu$ A and 300  $\mu$ A, respectively. The measured I-V characteristic fitted the exponential diode model very well (diode voltage within  $\pm 1$  mV to the model). When the diode was cooled to 20.7K, its series resistance rose by 3  $\Omega$  ( $R_s = 14.7 \Omega$ ), while the saturation current dropped to  $1.9 \times 10^{-52}$  A. The ideality factor increased to 5.34 ( $V_o = 9.5$  mV), and  $\Delta V$  was 24.1 mV. The exponential diode model did not describe the diode as well as at room temperature (up to 5 mV difference in diode voltage). The most significant effect observed in the diode upon cooling was the decrease of the equivalent I.F. noise temperature.  $T_{DC}$  was reduced approximately a factor of 4, being 50K and 57K at bias currents of 10  $\mu$ A and 300  $\mu$ A, respectively.

#### B. Measurements at Constant Temperature

Different criteria may be applied in optimizing the operation of the measurement system if the temperature of the mixer is constant or varies very slowly. The accuracy of measurements is of primary importance while the speed is no longer a limiting factor. Thus, more complexity and versatility both in testing and data processing is permissible and more information may be printed out between measurements. Therefore, the software used in mixer testing at



TEMPERATURE 293.2 K

TEMPERATURE 20.7 K

Fig. 8. Plots produced during cooling of the W-band Schottky diode mixer described in the text. Only measurements at the first (room) temperature and the last (20.7K) temperature are presented. Diode voltage,  $V_D$ , and equivalent I.F. noise temperature,  $T_{DC}$ , are measured and plotted versus D.C. bias current  $I_D$ . The computer fits measured  $V_D$  to an exponential diode model response and plots residuals of the fit,  $V_D - V_{FIT}$ . It also computes and plots derivatives  $dV_D(I_D)/d\log(I_D)$  and  $d[V_D(I_D) - I_D R_S]/d\log(I_D)$ . The latter is independent of  $\log(I_D)$  for an ideal exponential diode.

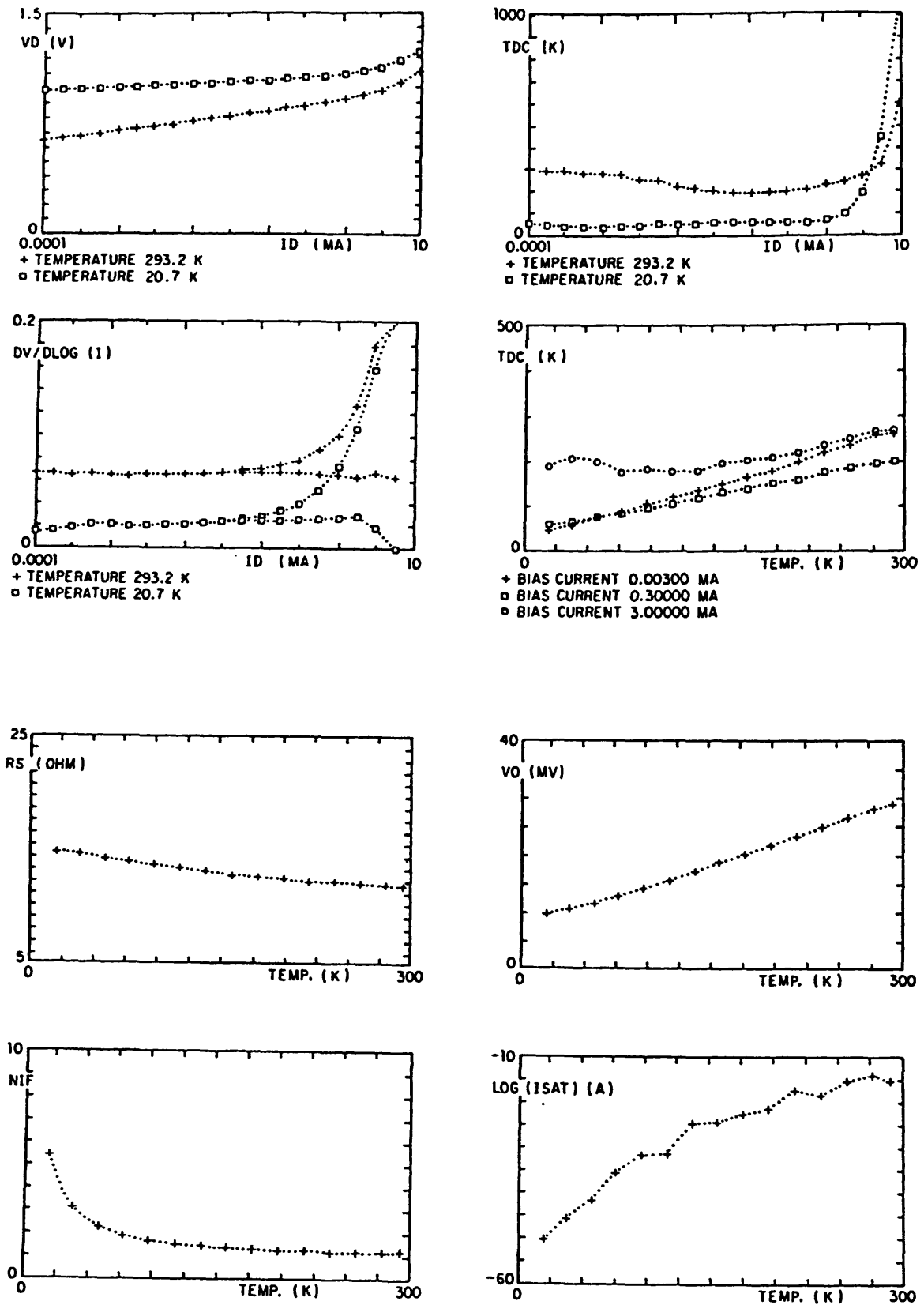


Fig. 9. Plots resulting from processing data collected during cooldown. Diode I-V characteristics and  $T_{DC}$  noise temperatures are compared at two temperatures. Measured  $T_{DC}$  is also plotted versus temperature for three bias currents. Diode series resistance  $R_S$ , ideality factor  $\eta$  (NIF),  $V_0 = \eta kT/q$  and saturation current  $I_{sat}$  are plotted versus temperature.



constant temperature includes also I-V characteristic and  $T_{DC}$  measurements, but different measurement loops are now employed. The equivalent I.F. noise temperature of the mixer with D.C. bias only,  $T_{DC}$ , may be measured not only at fixed I.F. frequency, but also with the I.F. swept from 1 GHz to 2 GHz in steps preset by the software. However, only that section of the software that supervises tests performed on the mixer with the L.O. signal applied will be detailed here.

The I.F. radiometer/reflectometer calibration is performed as described previously. To start the pumped mixer tests (Figure 10), the R.F. components and I.F. cable losses, necessary for computation of the corrections derived in Section II, are entered into the computer.

Mixer noise temperature and conversion loss may be measured at fixed I.F. frequency and also with I.F. center frequency swept from 1 GHz to 2 GHz in preprogrammed steps. At a given frequency and level of the millimeter-wave local oscillator signal and for given D.C. mixer diode bias, the I.F. frequency is swept three times as indicated in Figure 10. In the first and second sweeps, the R.F. hot load is in front of the mixer input while in the third sweep the R.F. cold load is seen by the mixer. The I.F. reflectometer noise source is turned on during the second sweep only. The mixer noise temperature and conversion loss are calculated and plotted versus I.F. during the last sweep. At the end of the measurement loop the plot and the mixer parameters may be printed out on request.

A subsequent measurement loop operates in a similar way except that the I.F. frequency is kept constant (default I.F.= 1.4 GHz).

The results of the measurements may be further processed with the aid of the computer which provides an easy and convenient means for optimizing, characterizing and documenting the R.F. performance of the mixer.

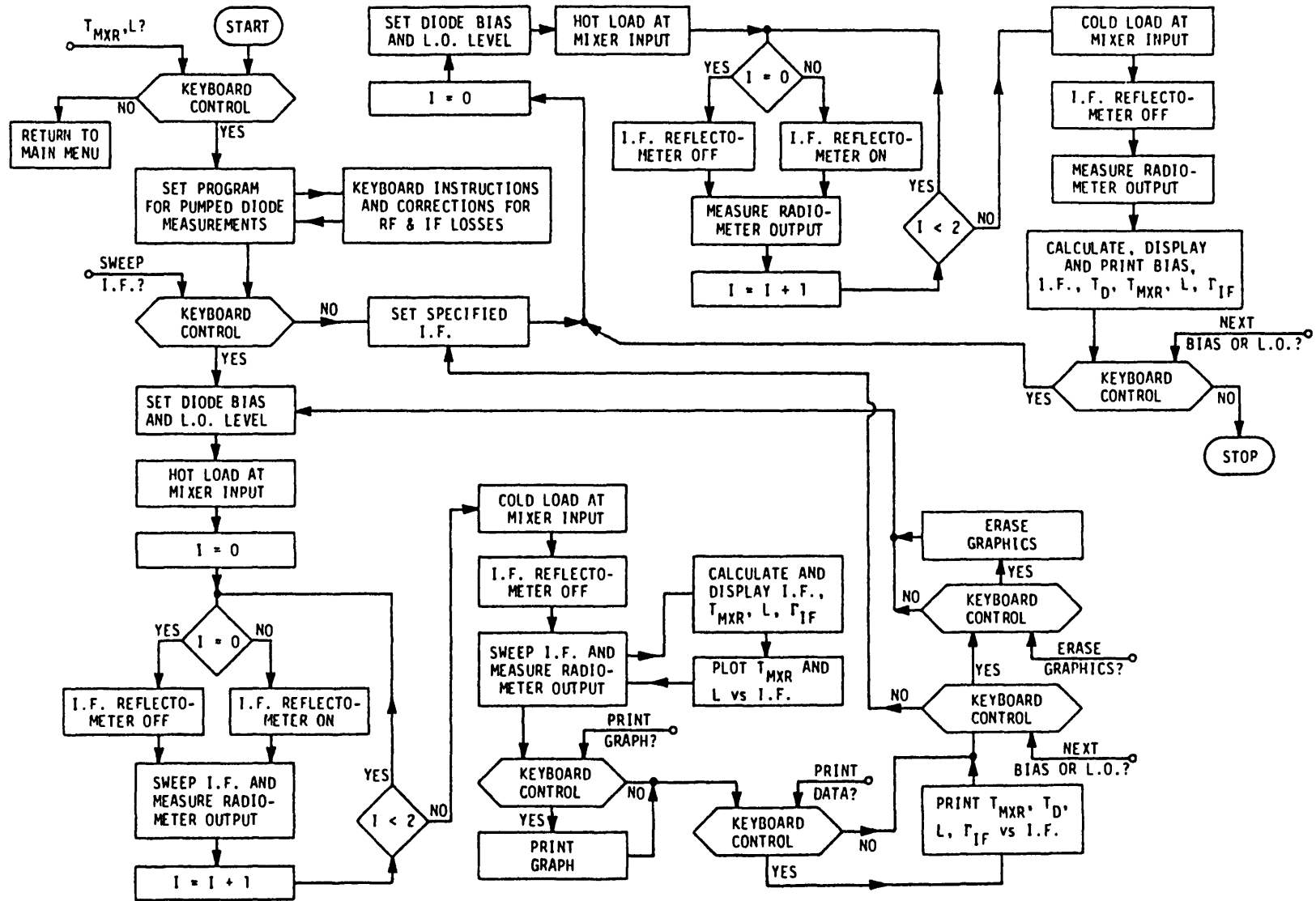


Fig. 10. Simplified block diagram of the software controlling the measurements and data processing at constant temperature.

The R.F. performance of the mixer, whose D.C. characteristics were described in the preceding section, was measured at a temperature of 24K for L.O. frequency varied from 96 GHz to 120 GHz. All single-sideband (SSB) values quoted assume equal sideband losses and are based on double-sideband measurements. The sideband losses for the mixer reported here have been measured and found to be equal to within five percent. The accuracy of the reported results is estimated to be  $\pm 3K$  and  $\pm 0.1$  dB in SSB mixer noise temperature and conversion loss, respectively.

The tuning of the mixer, once optimized, was fixed and only the quasi-optical diplexer was adjusted at each L.O. frequency using the mixer noise monitoring system implemented in the I.F. radiometer (Figure 4).

The mixer diode bias was kept constant at 0.94 V for each measurement frequency and L.O. level was adjusted to result in 0.36 mA D.C. component of the diode current. Using the radiometer monitoring system these operating conditions were found to result in the lowest mixer noise temperature. This is confirmed in Figure 11 in which single-sideband mixer noise temperature and conversion loss are plotted versus D.C. component of the diode current. The measurements were made at a temperature of 24K, an L.O. frequency of 110 GHz and I.F. = 1.45 GHz with 60 MHz measurement bandwidth. The minimum SSB mixer noise temperature of 81K was obtained at L.O. level (D.C. diode current of 0.36 mA) lower than that ( $I_{MXR} = 1.2$  mA) required for minimum conversion loss. The sharp minimum measured for the cryogenic mixer is much more distinct than the flat minimums in both mixer noise temperature and conversion loss usually observed for room temperature mixers at approximately the same L.O. levels. Thus more care is needed in optimizing the operating conditions of cryogenic mixers than for room temperature mixers.

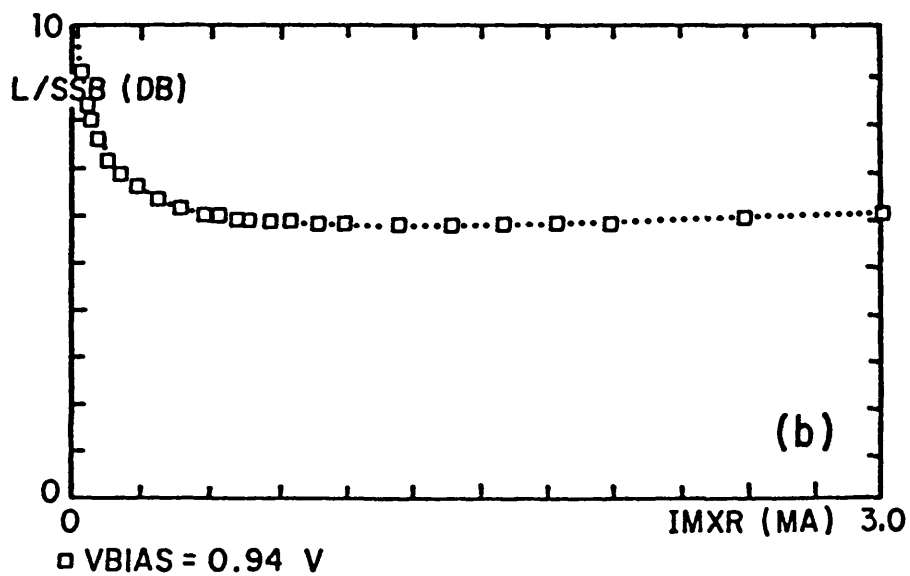
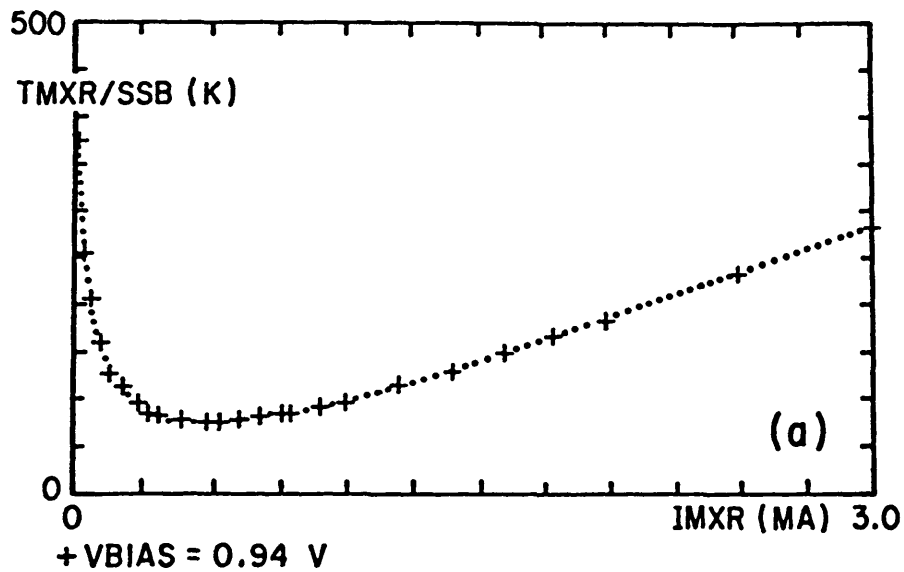


Fig. 11. Single-sideband mixer noise temperature,  $T_{MXR}$ , and corresponding single sideband conversion loss,  $L$ , of the mixer as a function of L.O. level. The L.O. level is represented by the D.C. component,  $I_{MXR}$ , of the diode current resulting from the applied L.O. signal. (Temp. = 24K,  $f_{LO} = 110$  GHz, I.F. = 1.45 GHz,  $\Delta f_{IF} = 60$  MHz, equal sideband losses).

At each L.O. frequency mixer noise temperature and conversion loss were measured as a function of I.F. frequency. The measurements were made at temperature of 24K and the I.F. measurement bandwidth was 60 MHz in all measurements.

The computer printout resulting from measurements at 110 GHz is shown in Figure 12. The SSB mixer noise temperature reaches 81K with the corresponding conversion loss of 5.7 dB at I.F. frequency of 1.45 GHz. The bandwidth over which the mixer noise temperature varies by less than 20% is at least 400 MHz. The I.F. response at other L.O. frequencies within the operating range is similarly broad.

#### V. Discussion of the Results

The performance of the mixer is summarized in Table I and illustrated in Figure 13 which was obtained as a result of data processing after the measurements. The single-sideband mixer noise temperature is less than 140K between 98 and 118 GHz and is  $81 \pm 3K$  with corresponding SSB conversion loss of  $5.7 \pm 0.1$  dB at L.O. frequency of 110 GHz. When evaluating this result, it should be noted that a fixed-tuned mixer of similar design can be optimized for low-noise performance in a broader R.F. frequency range if higher noise temperature is acceptable. ( $T_M^{SSB} \approx 150K$  in the 85-120 GHz frequency range was reported in [24].

The filled square in Figure 13 represents the lowest mixer noise temperature ever reported for a Schottky diode, W-band mixer [38]. That result was derived from DSB measurements of a receiver which was tuned at each frequency. The derivations were made only at the frequency of 101 GHz at which SSB mixer noise temperature of 70K was specified. The results reported in this paper are direct measurements of the mixer noise temperature and conversion loss of the fixed-tuned, fixed-bias mixer (i.e., no tuning or adjustments of the mixer were made when the

TABLE I - R.F. PERFORMANCE OF THE FIXED-TUNED MIXER

$F_{LO}$ [GHz]	$T_M^{SSB}$ [K]	$L_c^{SSB}$ [dB]	$ \Gamma_{IF} ^2$
96.0	177	6.4	0.009
98.0	133	6.2	0.017
100.0	126	6.2	0.018
102.0	135	6.1	0.009
104.0	118	6.1	0.013
106.0	113	5.9	0.010
108.0	85	5.8	0.015
109.0	81	5.9	0.010
110.0	81	5.7	0.007
112.0	95	5.8	0.007
113.5	106	5.8	0.011
115.0	104	5.9	0.031
116.0	123	6.2	0.027
118.0	139	7.2	0.104
120.0	306	8.7	0.259

NOTE: Diode bias 0.94 V, D.C. diode current 0.36 mA. Temp. = 24K,  
I.F. = 1.45 GHz,  $\Delta f_{IF} = 60$  MHz. Equal sideband losses.

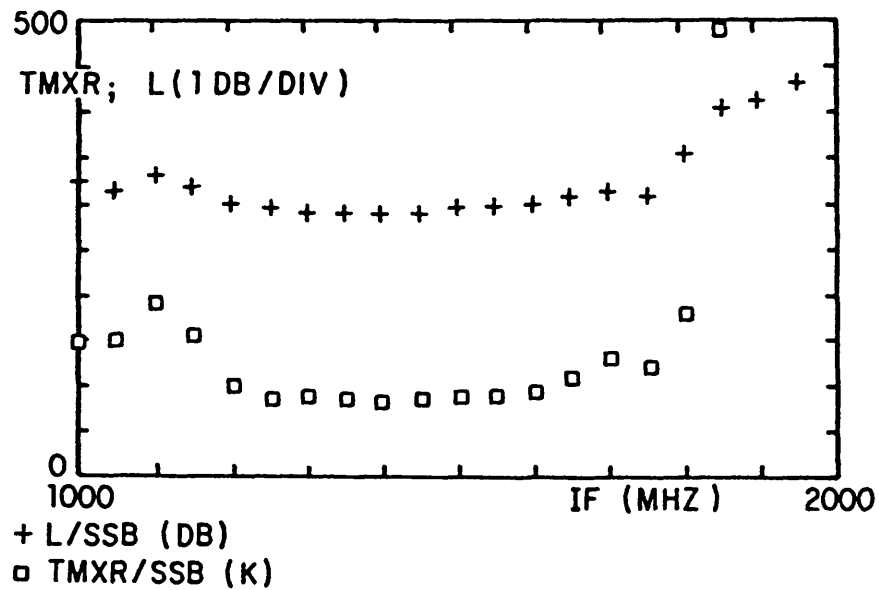


Fig. 12. Single-sideband mixer noise temperature,  $T_{MXR}$ , and corresponding single-sideband conversion loss,  $L$ , of the mixer versus I.F. frequency. (Temp. = 24K,  $f_{LO} = 110$  GHz,  $\Delta f_{IF} = 60$  MHz,  $V_D = 0.94V$ ,  $I_{MXR} = 0.36$  mA, equal sideband losses).

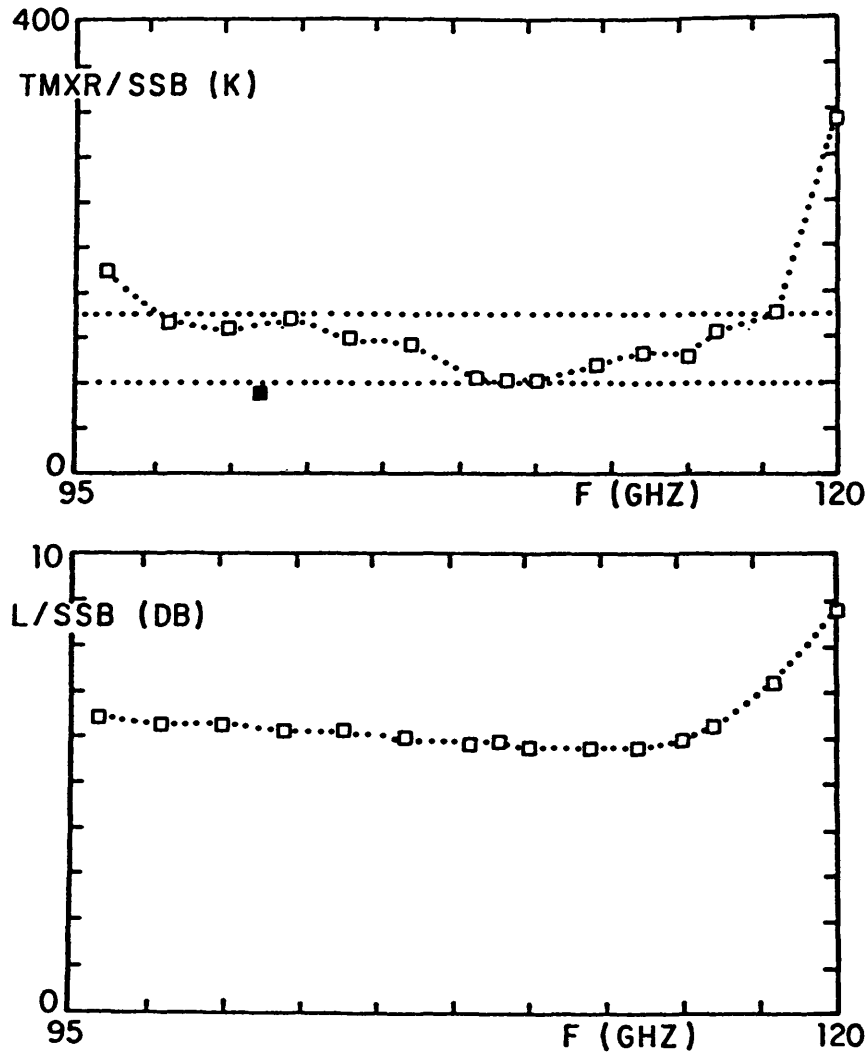


Fig. 13. Single-sideband mixer noise temperature,  $T_{MXR}$ , and corresponding single-sideband conversion loss,  $L$ , of the mixer versus L.O. frequency. (Temp. = 24K, I.F. = 1.45 GHz,  $\Delta f_{IF} = 60$  MHz,  $V_D = 0.94$  V,  $I_{MXR} = 0.36$  mA, equal sideband losses).



frequency was varied) optimized for best performance in the 20 GHz R.F. frequency bandwidth.

To further illustrate the usefulness of accurate mixer characterization and to evaluate the excellent result obtained with the reported mixer, it is useful to examine how the mixer performance compares with the fundamental limits imposed on a Schottky barrier diode mixer. In order to do that, it is necessary to determine contributions to the mixer noise from the diode itself and from the lossy mount. The measured total conversion loss  $L_c^{DSB}$  is composed of:  $L_{RF}$ , the losses in the scalar feed, input quarter-wave transformer, reduced height waveguide and fixed backshort;  $L_D$ , the diode conversion loss; and  $L_{IF}$ , the losses in the output microstrip choke and I.F. transformer. Because at 110 GHz measured  $|\Gamma_{IF}|^2 = 0.007$  then from equation (32)  $L_c^{DSB} \approx L_a^{DSB}$  and

$$L_a^{DSB} = L_{RF} L_D L_{IF} \cdot \quad (36)$$

The mount R.F. and I.F. losses at cryogenic temperatures can only be estimated from room temperature data on the basis of the increase in the conductivity of OFHC copper and the gold plating upon cooling. At room temperature scalar feed loss is 0.1 dB, the input waveguide transformer is assumed to have a loss of 0.25 dB and the reduced height waveguide and fixed backshort, 0.1 dB. The sum of these losses is assumed to decrease to  $0.25 \pm 0.05$  dB when cooled. The I.F. losses are assumed to decrease upon cooling from 0.2 dB to  $0.15 \pm 0.05$  dB. At a physical temperature of  $T = 24K$ , the diode conversion loss,  $L_D$ , may then be estimated from the measured data and equation (36) to be between 2.15 dB and 2.45 dB at a frequency of 110 GHz.

The total DSB mixer noise temperature is

$$T_M^{DSB} = (L_{RF} - 1)T + L_{RF}(L_D - 1)T_{eq} + L_{RF}L_D(L_{IF} - 1)T \quad (37)$$

The equivalent temperature  $T_{eq}$  of the diode as a lossy element is limited by

$$T_D = \frac{\eta T}{2} \quad (38)$$

derived in [21]. This only applies to a pumped ideal resistive exponential diode ( $R_s = 0$ ,  $C_j = \text{const}$ ) operating as a mixer, for the case where higher harmonics are reactively terminated and only shot-noise is generated by the diode.

The Schottky diode used in the mixer, at a temperature of 24K was characterized by an ideality factor  $\eta = 4.3 \pm 0.1$ . This results in a shot-noise limit of  $T_D = 51.6 \pm 1.2\text{K}$  which is used in equation (37) to derive limits for the mixer noise temperature. The results obtained for the shot-noise limited mixer diode embedded in lossy and lossless mount ( $L_{RF} \rightarrow 0 \text{ dB}$ ,  $L_{IF} \rightarrow 0 \text{ dB}$ ) are compared in Table II to the measured performance of the practical mixer. The noise temperatures of the reported mixer and the lossy mount model are equal to within the accuracy of measurements and uncertainty of derivations. This demonstrates that, through careful mount and diode development and optimization, it is possible to construct a W-band mixer which approaches the shot-noise limited ideal case, i.e., the diode series resistance and parametric effects due to the diode nonlinear capacitance are negligible, higher harmonics are reactively terminated, there is no excess noise in the diode, and correlated shot-noise components from high harmonics are minimized. The noise of the mixer is determined by the shot-noise generated in the diode and mount losses contribute only  $\approx 9\text{K}$  to the SSB mixer noise temperature (6.4K and 2.6K due to R.F. and I.F. losses, respectively).

LIMITS IMPOSED ON SCHOTTKY DIODE MIXER

PRACTICAL MIXER	<p>MEASUREMENTS OF THE D.C. BIASED DIODE</p> <p><math>I_D = 360 \mu\text{A}</math></p> <p>Temp. = 24K</p>	<p><math>\eta = 4.3 \pm 0.1</math></p> <p><math>R_S = 14.7 \pm 0.1 \Omega</math></p> <p><math>T_{DC} = 61 \pm 3K</math></p>
	<p>MEASURED MIXER PERFORMANCE</p> <p><math>F_{LO} = 110 \text{ GHz}</math></p> <p>Temp. = 24K</p>	<p><math>L_c^{SSB} = 5.7 \pm 0.1 \text{ dB}</math></p> <p><math> \Gamma_{IF} ^2 = 0.007</math></p> <p><math>T_M^{SSB} = 81 \pm 3K</math></p>
MODEL A	<p>SHOT NOISE LIMITED MIXER LOSSLESS MOUNT</p> <p><math>L_{RF} = 0 \text{ dB}</math></p> <p><math>L_{IF} = 0 \text{ dB}</math></p>	<p><math>L_c^{SSB} = 2L_D</math></p> <p><math>T_D = 51.6 \pm 1.2K</math></p> <p><math>5.16 \text{ dB} \leq L_c^{SSB} \leq 5.46 \text{ dB}</math></p> <p><math>64.6K \leq T_M^{SSB} \leq 80.0K</math></p>
MODEL B	<p>SHOT NOISE LIMITED MIXER LOSSY MOUNT</p> <p><math>L_{RF} = 0.25 \pm 0.05 \text{ dB}</math></p> <p><math>L_{IF} = 0.15 \pm 0.05 \text{ dB}</math></p>	<p><math>L_c^{SSB} = 5.7 \pm 0.1 \text{ dB}</math></p> <p><math>T_D = 51.6 \pm 1.2K</math></p> <p><math>2.15 \text{ dB} \leq L_D \leq 2.45 \text{ dB}</math></p> <p><math>76.4K \leq T_M^{SSB} \leq 88.2K</math></p>

Measured mixer performance is compared to limits [21] established for an ideal exponential resistive diode generating shot-noise only and operating as a mixer in which higher harmonics are reactively terminated. The diode is embedded in a lossless mount (Model A) and in a mount having losses equal to the losses of the practical mixer mount (Model B).

## VI. Summary

The theory for accurate measurements of millimeter-wave mixers has been presented clarifying some common misunderstandings and misinterpretations. The corrections that need to be applied in order to accurately determine mixer parameters from measured quantities have been derived and sources of potential measurement inaccuracies inherent in the hot/cold load measurement technique have been indicated.

Two computerized measurement systems operating on the basis of this theory have been constructed to allow testing of millimeter wave mixers in the frequency range from 90 GHz to 350 GHz. The design criteria and descriptions of both the hardware and the software have been given. The measurement systems have been extensively used in testing of millimeter wave mixers, e.g., [24], [39], [40] and have been an essential and invaluable asset in mixer development.

A W-band, ultra low-noise mixer has been selected to illustrate the operation of the measurement system and to show the versatility and thoroughness of the available tests, which in many cases would not be feasible without the aid of a computer. The fixed-tuned, fixed-bias mixer used as an illustrative example in this paper has a single sideband noise temperature less than 140K between 98 and 118 GHz and at 110 GHz achieves shot-noise limited performance with a SSB noise temperature of only 81K and corresponding conversion loss of 5.7 dB.

## VII. Acknowledgements

The authors are grateful to W. Luckado, G. Taylor and D. Dillon for their excellent work in fabricating the many components of the measurement systems. Thanks also go to N. Horner, Jr. for his assembly of the mixer and frequency multipliers. Prof. R. Mattauch of the University of Virginia is thanked for supplying the Schottky barrier diodes.

## REFERENCES

- [1] J. M. Kenney, "The Simultaneous Measurement of Gain and Noise Using Only Noise Generators," IEEE Trans. Microwave Theory Tech., vol. MTT-16, no. 9, pp. 603-607, Sept. 1968.
- [2] M. Akaike and S. Okamura, "Semiconductor Diode Mixer for Millimeter-Wave Region," Electron. Commun. (Japan), vol. 52-B, pp. 84-93, 1969.
- [3] S. Weinreb and A. R. Kerr, "Cryogenic Cooling of Mixers for Millimeter and Centimeter Wavelengths," IEEE J. Solid-State Circuits, vol. SC-8, no. 1, pp. 58-63, Feb. 1973.
- [4] A. R. Kerr, "Low-Noise, Room Temperature and Cryogenic Mixers for 80-120 GHz," IEEE Trans. Microwave Theory Tech., vol. MTT-23, no. 10, pp. 781-787, Oct. 1975.
- [5] A. R. Kerr, R. J. Mattauch and J. A. Grange, "A New Mixer Design for 140-220 GHz," IEEE Trans. Microwave Theory Tech., vol. MTT-25, no. 5, pp. 399-401, May 1977.
- [6] H. Cong, A. R. Kerr and R. J. Mattauch, "The Low-Noise 115 GHz Receiver on the Columbia-GISS 4-ft. Radio Telescope," IEEE Trans. Microwave Theory Tech., vol. MTT-27, no. 3, pp. 245-248, March 1979.
- [7] J. W. Archer and R. J. Mattauch, "Low Noise, Single-Ended Mixer for 230 GHz," Electronics Letters, vol. 17, no. 5, pp. 180-181, 5 March 1981.
- [8] J. W. Archer, "All Solid-State, Low-Noise Receivers for 210-240 GHz," IEEE Trans. Microwave Theory Tech., vol. MTT-30, no. 8, pp. 1247-1252, August 1982.
- [9] N. R. Erickson, "A Cryogenic Receiver for 1 mm Wavelength," 6th Int. Conf. Infrared Millimeter Waves Dig., p. W-3-7, Dec. 1981.

- [10] B. Vowinkel, K. Gr<sup>u</sup>ner, H. S<sup>u</sup>ss and W. Reinert, "Cryogenic All Solid-State Millimeter Wave Receivers for Airborne Radiometry," 1983 IEEE MTT-S Int. Microwave Symp. Dig., pp. 566-568, May 1983.
- [11] E. R. Carlson, M. V. Schneider and T. F. McMaster, "Subharmonically Pumped Millimeter-Wave Mixers," IEEE Trans. Microwave Theory Tech., vol. MTT-26, no. 10, pp. 706-715, Oct. 1978.
- [12] E. L. Kollberg and H. H. G. Zirath, "A Cryogenic Millimeter-Wave Schottky Diode Mixer," IEEE Trans. Microwave Theory Tech., vol. MTT-31, no. 2, pp. 230-235, Feb. 1983.
- [13] N. Keen and S. Lidholm, "K Factor Simplifies Chopped Noise Readings," Microwaves, p. 59, April 1981.
- [14] R. Trambarulo and H. S. Berger, "Conversion Loss and Noise Temperature of Mixers from Noise Measurements," 1983 IEEE MTT-S Int. Microwave Symp. Dig., pp. 364-365, May 1983.
- [15] C. T. Stelzried, "Microwave Thermal Noise Standards," IEEE Trans. Microwave Theory Tech., vol. MTT-16, no. 9, pp. 646-654, Sept. 1968.
- [16] A. R. Kerr, "The Thermal Noise of Lossy Cables Used in Noise Measurements," NASA/Goddard Institute For Space Studies Internal Report, New York, Dec. 1980.
- [17] "Description of the Noise Performance of Amplifiers and Receiving Systems," Proc. IEEE, vol. 51, no. 3, pp. 436-442, March 1963.
- [18] A. V. R<sup>a</sup>is<sup>a</sup>nen, "Formulas for the Noise Temperature and Noise Figure of a Mixer and a Heterodyne Receiver Derived from the Basic Noise Figure Definition," Five College Radio Astronomy Observatory Report No. 132, University of Massachusetts, Amherst, 1979.

- [19] T. Y. Otoshi, "The Effect of Mismatched Components on Microwave Noise Temperature Calibrations," IEEE Trans. Microwave Theory Tech., vol. MTT-16, no. 9, pp. 675-686, Sept. 1968.
- [20] H. Fukui, "Available Power Gain, Noise Figure and Noise Measure of Two-Ports and Their Graphical Representations," IEEE Trans. Circuit Theory, vol. CT-13, no. 2, pp. 137-142, June 1966.
- [21] A. R. Kerr, "Shot-Noise in Resistive Diode Mixers and the Attenuator Noise Model," IEEE Trans. Microwave Theory Tech., vol. MTT-27, no. 2, pp. 135-140, Feb. 1979.
- [22] J. W. Archer, "A Multiple Mixer, Cryogenic Receiver for 200-350 GHz," Rev. of Sci. Instruments, vol. 54, no. 10, pp. 1371-1376, Oct. 1983.
- [23] D. H. Martin and E. Puplett, "Polarized Interferometric Spectroscopy for the Millimeter and Submillimeter Spectrum," Infrared Phys., vol. 10, pp. 105-109, 1969.
- [24] J. W. Archer and M. T. Faber, "A Very Low-Noise Receiver for 80-120 GHz," Int. J. Infrared Millimeter Waves, vol. 5, no. 8, pp. 1069-1081, August 1984.
- [25] J. W. Archer and M. T. Faber, "Low-Noise, Fixed-Tuned, Broadband Mixer for 200-270 GHz," Microwave Journal, no. 7, pp. 135-142, July 1984.
- [26] J. Silver, "Microwave Antenna Theory and Design," M.I.T. Rad. Lab Series, vol. 12, ch. 11, New York: McGraw-Hill, 1949.
- [27] J. W. Archer and M. T. Faber, "A Simple Model for Computer-Aided Analysis and Design of Grooved Dielectric Panels and Lenses," in preparation, June 1985.
- [28] J. W. Archer, "A High Performance Frequency Doubler for 80 to 120 GHz," IEEE Trans. Microwave Theory Tech., vol. MTT-30, no. 5, pp. 824-825, May 1982.

- [29] J. W. Archer, "Millimeter Wavelength Frequency Multipliers," IEEE Trans. Microwave Theory Tech., vol. MTT-29, no. 6, pp. 552-557, June 1981.
- [30] J. W. Archer, "An Efficient 200-290 GHz Frequency Tripler Incorporating a Novel Stripline Structure," IEEE Trans. Microwave Theory Tech., vol. MTT-32, no. 4, pp. 416-420, April 1984.
- [31] J. W. Archer, "A Novel Quasi-Optical Frequency Multiplier Design for Millimeter and Submillimeter Wavelengths," IEEE Trans. Microwave Theory Tech., vol. MTT-32, no. 4, pp. 421-427, April 1984.
- [32] J. W. Archer and M. T. Faber, "High-Output, Single- and Dual-Diode, Millimeter-Wave Frequency Doublers," IEEE Trans. Microwave Theory Tech., vol. MTT-33, no. 6, pp. 533-538, June 1985.
- [33] S. Weinreb, D. L. Fenstermacher and R. Harris, "Ultra Low-Noise, 1.2-1.7 GHz, Cooled GaAs FET Amplifiers," IEEE Trans. Microwave Theory and Tech., vol. MTT-30, no. 6, pp. 849-853, June 1982.
- [34] S. Weinreb, 1982, private communication.
- [35] G. Weinreb and S. Weinreb, "ADIOS - Analog-Digital Input Output System for Apple Computer," National Radio Astronomy Observatory, Electronics Division Internal Report No. 212, April 1981.
- [36] D. N. Held and A. R. Kerr, "Conversion Loss and Noise of Microwave and Millimeter-Wave Mixers: Part 1 - Theory," and "Part 2 - Experiment," IEEE Trans. Microwave Theory Tech., vol. MTT-26, no. 2, pp. 49-61, Feb. 1978.
- [37] M. T. Faber and W. K. Gwarek, "Nonlinear-Linear Analysis of Microwave Mixer with Any Number of Diodes," IEEE Trans. Microwave Theory Tech., vol. MTT-28, no. 11, pp. 1174-1181, Nov. 1980.



- [38] C. R. Predmore, A. V. Räsänen, N. R. Erickson, P. F. Goldsmith and J. L. R. Marrero, "A Broadband, Ultra Low-Noise, Schottky Diode Mixer Receiver from 80 to 115 GHz," IEEE Trans. Microwave Theory Tech., vol. MTT-32, no. 5, pp. 498-506, May 1984.
- [39] J. W. Archer and M. T. Faber, "Low-Noise, Fixed-Tuned, Broadband Mixer for 200-270 GHz," 1984 IEEE MTT-S Int. Microwave Symp. Dig., pp. 557-559, May 1984.
- [40] M. T. Faber and J. W. Archer, "A Very Low-Noise, Fixed-Tuned Mixer for 240-270 GHz," 1985 IEEE MTT-S Int. Microwave Symp. Dig., pp. 311-314, June 1985.

